



**The Abdus Salam
International Centre for Theoretical Physics**



2015-11

**Joint ICTP/IAEA Workshop on Advanced Simulation and Modelling
for Ion Beam Analysis**

23 - 27 February 2009

Data analysis software for ion beam analysis

N.P. Barradas
*Instituto Tecnológico e Nuclear
Portugal*

E. Rauhala
*University of Helsinki
Finland*

Data analysis software for ion beam analysis

N.P. Barradas

Instituto Tecnológico e Nuclear , Estrada Nacional No. 10, Apartado 21, 2686-953 Sacavém, Portugal.

Centro de Física Nuclear da Universidade de Lisboa, Av. Prof. Gama Pinto 2, 1649-003 Lisboa, Portugal.

E. Rauhala

Accelerator Laboratory, Dept. of Physical Sciences, University of Helsinki, P.O. Box 64, FIN-00014 Helsinki, Finland.

Contents

1. Introduction

- 1.1. Data analysis software
- 1.2. Scope of the chapter
- 1.3. Historical development and reviews of software programs

2. Types of codes

- 2.1 The direct calculation method
- 2.2 Simulation by successive iterations
- 2.3 Interactive vs. automated
- 2.4 Deterministic vs. Stochastic (Monte Carlo)

3. Capabilities of codes

- 3.1 Design basis
 - 3.1.1 Techniques implemented
 - 3.1.2 Experimental conditions supported
 - 3.1.3 Description of samples
- 3.2 Data bases implemented
 - 3.2.1 Stopping power
 - 3.2.2 Scattering cross section
- 3.3 Basic physics
- 3.4 Advanced physics
 - 3.4.1 Straggling models
 - 3.4.2 Electron screening
 - 3.4.3 Plural scattering
 - 3.4.4 Multiple scattering
 - 3.4.5 Simulation of resonances
 - 3.4.6 Surface and interface roughness

- 3.4.7 Channeling
- 3.4.8 Pulse pile-up
- 3.5 Automated optimization
 - 3.5.1 Fitting
 - 3.5.2 Bayesian inference
- 3.6 Usability and usage
- 3.6 Accuracy of codes

4. Accuracy

- 4.1 Numerical accuracy of codes
- 4.2 Intrinsic accuracy of IBA experiments
 - 4.2.1 Models and basic physical quantities
 - 4.2.2 Experimental conditions
 - 4.2.3 Counting statistics
- 4.3 Physical effects on data analysis

5. RUMP and first generation codes

6. New generation codes - SIMNRA and NDF

- 6.1 Further capabilities
- 6.2 SIMNRA
- 6.3 NDF
- 6.4 Issues

7. Monte Carlo simulation

8. Other techniques

- 8.1 PIXE
- 8.2 Resonant NRA, PIGE, NRP, MEIS, channeling, microscopies, etc.

1. Introduction

1.1. Data analysis software

The data analysis software in ion beam methods are computer programs designed to extract information about the sample from the measured ion beam spectra. The desired information includes identification of sample elements, their concentrations, areal densities and thicknesses of layers. At best, one spectrum can be converted to concentration depth distributions of all elements in the sample. Often, however, such a full description of the sample based on a single experiment is not possible. The analyst can then perform additional experiments with different experimental parameters such as ion energies, different measurement geometry, use another ion beam technique, or include information from other complementary techniques.

The software can also be used for designing relevant experiments. Depending on the assumed sample structure, the appropriate ion beam technique can be chosen by doing test simulations prior to experiments. The most suitable parameters for the measurements may be tested. The choice of ions, energies, geometries etc. may be examined without performing often extensive and complicated experiments.

The third main function of the software is found in education and research. By using simulation computer programs, the researcher may readily scrutinize the characteristics of various ion beam techniques. The dependencies between stopping powers, cross sections, energies, etc. can be studied. Novel reaction cross sections and stopping powers may be implemented in the program to investigate the agreement between simulation and experimental data. Fine details, such as double and multiple scattering, screening, pile-up, properties of various detector systems, etc. may be analyzed with the help of data analysis programs.

It cannot be overemphasized that software is an aide to data analysis, and does not replace the judgment of the analyst. Software that is not correctly used, or used outside its scope of application, leads to wrong data analysis. Furthermore, it should be noted that the scope of application of a given program may not be clear and depends on the details of the experiment being analyzed: for instance, Bohr straggling is adequate for analysis of normal incidence proton-RBS with a surface barrier detector, but completely inadequate for heavy ion ERDA or for high resolution near-surface analysis where the straggling is asymmetric.

1.2. Scope of the chapter

This chapter deals mainly with the data analysis software of particle-particle ion beam analysis (IBA) techniques, Rutherford backscattering spectrometry (RBS), Elastic recoil detection analysis (ERDA) and nuclear reaction analysis (NRA). The last case we limit ourselves to techniques utilizing one single beam energy, as opposed to resonant NRA or narrow resonance profiling (NRP) (see Amsel, 1996, for a discussion on acronyms). Short sections on PIXE and other techniques such as NRP and channeling are also included.

1.3. Historical development and reviews of software programs

Computer programs to analyze data from RBS, NRA, and ERDA date back to the 1960's and 1970's. These techniques developed parallel to the beginning of the new semiconductor and

other high-tech technologies, where new needs of ion beams in the production, modification and characterization of novel materials were arising. The IBA techniques for quantitative depth profiling in the micron range and determination of low-concentration elemental impurities were quickly recognized and widely applied. As these analytical tools became more versatile, also the samples, spectra and data analysis problems became more complicated. By the end of the 1990s, the codes had developed in various directions; codes exist which can handle very general data analysis problems and various IBA techniques, some are highly automatic, others treat specified problems with great exactness.

The historical development of the software has been reviewed recently in Rauhala et al. (2006). This article also presents the characteristics and status of 12 software packages in 2006. An intercomparison of several software packages for simulations and real data analysis applications is presented in Barradas et al. (2007).

2. Types of codes

2.1 The direct calculation method

In direct spectrum analysis, the yield from separated signals of the spectrum is transformed into concentration values by closed form analytical calculation. Other forms of direct analysis include conversion from signal areas and heights to total amounts or concentrations. This is the opposite of spectrum simulation, where a theoretical spectrum is generated from an assumed depth profile and compared to the data.

This was introduced by Børgeesen et al. (1982) in the code SQUEAKIE. This approach is straightforward and effective in many cases. However, it has problems due to the implementation of straggling and the stability of results due to uncertainties in the stopping database and measurement noise. The direct method is still used, normally as a complement to full simulations, and often in heavy ion ERDA (Spaeth, 1998).

2.2 Simulation by successive iterations

Almost all of the presently available IBA data analysis software is based on simulation by successive iterations. The simulation modeling assumes that the underlying physics, mathematics and nuclear and atomic data are valid, and adequately describe the physical processes involved. Starting from a known sample structure, the corresponding experimental energy spectrum can be theoretically simulated from a few basic data, and the known formalism of the reaction spectrometry. Comparing the experimental and theoretical spectra, after a few iterations where the assumed composition of the sample is iteratively modified, a close similarity of the spectra is accomplished. The sample structure leading to the theoretical spectrum is then taken to correspond to the material's sample structure. Erroneous results or misinterpretations of the material's structure can result from incorrect science, ambiguous data, or inadequate software documentation and guidance for people to extract the correct information.

The typical iterative simulation proceeds as follows:

1. Assume the experimental parameters and the experimental spectrum known.
2. Assume an initial sample composition.

3. Calculate a theoretical spectrum corresponding to the experimental parameters and the sample composition to simulate the experimental spectrum.
4. Compare the simulated spectrum to the experimental spectrum.
5. Identify the differences and modify the assumed sample composition accordingly.
6. Repeat the iteration steps 3 – 5 until an adequate fit between the simulated and the experimental spectrum is accomplished.
7. The assumption of the sample parameters corresponding to the the best simulation is taken to be the sample structure resulting from the data analysis.

This procedure is illustrated in the **Worked example DA1 - Convergence of iteration.**

Worked example DA1: Convergence of iteration.

Assume that the experimental parameters and the elements in the sample are known. Start by making a guess about the sample composition. How do the iterations converge?

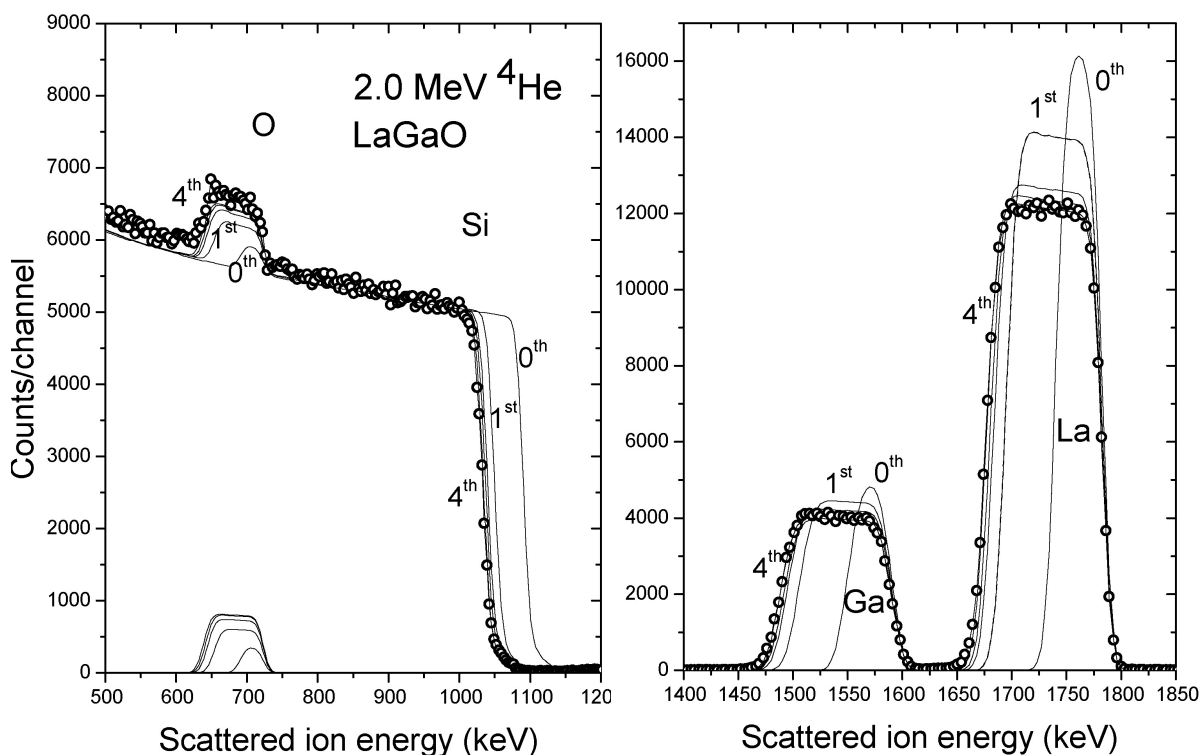


Fig. DA1. Backscattering spectrum (open circular symbols) for 2.00 MeV ^4He ions incident on a LaGaO layer on a silicon substrate

Fig. DA1 illustrates the spectrum for 2.00 MeV ^4He ions incident on a LaGaO layer on a silicon substrate. In the experiment, the following parameters have been used:

Incident ^4He -ion energy, $E_{\text{He}} = 2,00 \text{ MeV}$

Scattering angle $\theta = 170^\circ$
Angle of incidence $\theta_i = 50^\circ$
Solid angle \times accumulated charge $Q\Omega = 69.0 \text{ msr} \times \mu\text{C}$
Energy per channel $\delta E = 3.475 \text{ keV/ch}$
Energy in zero channel = 27.3 keV

Zeroth iteration

Initially, as a guess of the LaGaO film composition, equal concentrations of the elements in a layer of $200 \times 10^{15} \text{ at/cm}^2$ areal density were assumed.

Initial assumption:

Equal amounts of the three elements, 33% La, 33% Ga, 33% O
Layer areal density: $200 \times 10^{15} \text{ at/cm}^2$
 $\Rightarrow 0^{\text{th}}$ iteration

The resulting simulated spectrum is denoted as the 0^{th} iteration. The simulated signal heights of La and Ga and the signal width of La were then compared to those of the experimental spectrum. Concentrations and layer areal density were changed assuming the same linear dependence between signal heights and concentrations and between the signal widths and areal density of the layer.

The La concentration was thus multiplied by the ratio of experimental La signal height to simulated La signal height. Similarly, the areal density of the film was multiplied by the ratio of the experimental La signal width to the simulated La signal width.

This process was then repeated. The solid lines denoted as $1^{\text{st}}, \dots, 4^{\text{th}}$, in Figure X, show the results of subsequent iterations. In detail, the iteration converged as follows:

First iteration

The height of experimental La signal was observed to be roughly 75% of the height of the simulated signal. The same ratio for Ga was observed to be 80%.
The experimental La signal was observed to be roughly 2.4 times wider than the simulated signal.

Reduce the La concentration to $75\% \times 0.33 = 0.25$.

Reduce the Ga concentration to $80\% \times 0.33 = 0.26$.

Increase the areal density of the layer to $2.4 \times 200 \times 10^{15} \text{ at/cm}^2 = 480 \times 10^{15} \text{ at/cm}^2$.

\Rightarrow Iteration 1.

Second iteration

The height of experimental La signal was observed to be 85% of the height of the simulated signal. The same ratio for Ga was observed to be 88%.

The experimental signal was observed to be 1.2 times wider than the simulated signal.

Reduce the La concentration to $85\% \times 0.25 = 0.21$.

Reduce the Ga concentration to $88\% \times 0.26 = 0.23$.

Increase the areal density of the layer to $1.2 \times 480 \times 10^{15} \text{ at/cm}^2 = 580 \times 10^{15} \text{ at/cm}^2$.

⇒ Iteration 2.

Third iteration

The height of experimental La signal was observed to be 95% of the height of the simulated signal. The same ratio for Ga was observed to be 93%.

The experimental signal was observed to be 1.06 times wider than the simulated signal.

Reduce the La concentration to $95\% \times 0.21 = 0.20$.

Reduce the Ga concentration to $93\% \times 0.23 = 0.21$.

Increase the areal density of the layer to $1.06 \times 580 \times 10^{15} \text{ at/cm}^2 = 615 \times 10^{15} \text{ at/cm}^2$.

⇒ Iteration 3.

Fourth iteration

The height of experimental La signal was observed to be 97% of the height of the simulated signal. The Ga signal was fitted ok.

The experimental signal was observed to be 1.04 times wider than the simulated signal.

Reduce the La concentration to $97\% \times 0.20 = 0.195$.

The Ga concentration remains as 0.21.

Increase the areal density of the layer to $1.04 \times 615 \times 10^{15} \text{ at/cm}^2 = 640 \times 10^{15} \text{ at/cm}^2$.

⇒ Iteration 4.

As a result of the 4th iteration, both the signal heights and the signal widths of La and Ga seem to be fitted adequately within the plotting accuracy of the Figure.

In practical terms, the users tend to adjust the concentration and thickness values manually, without doing the exact procedure shown here. This leads to a larger number of iterations, which most users find acceptable given that the calculations are very fast with modern computers.

The crucial point in the iterative procedure is to describe the sample composition. Several codes let the user introduce functions that describe the depth profile of a given element. However, the most popular method to describe a sample is to divide it into sublayers. Each sublayer has a different composition, which is iteratively changed. Also, the number of sublayers is increased or decreased during the iterative procedure: if the current number of layer is not enough to reproduce the changing signals observed, the user introduces a new layer. If, on the other hand, the user can obtain an equivalent fit by using fewer layers, this is normally preferred. In practice, the depth resolution of the experiment limits the number of layers needed. This is illustrated in the **Worked example DA2 - Simulating composition changes by division into sublayers**.

Worked example DA2: Simulating composition changes by division into sublayers.

Changes of concentrations of components within a layer may be treated by dividing the layer into sublayers in which the composition remains constant. **Fig. DA2** shows a spectrum for

2.75 MeV ^7Li ions incident on a PbZrSnO thin-film sample on a Si substrate (Harjuoja et al, 2006). When trying to simulate the spectrum one finds that the interface between the film and the substrate is not well defined and that the concentrations change with depth within the thin film.

This has been simulated by assuming 9 sublayers of constant composition. The simulated spectrum as a result of data analysis by GISA is illustrated as the thick solid line connecting the experimental data points. The theoretical signals of the elemental components in each of the sublayers are shown as thin solid lines. The thick solid line thus represents the sum of the thin lines of the elemental signals in the sublayers.

The experimental parameters, the concentrations of the elements and the areal densities of the sublayers are given in the table below. The concentrations of the elements versus areal density are shown in **Fig. DA3**.

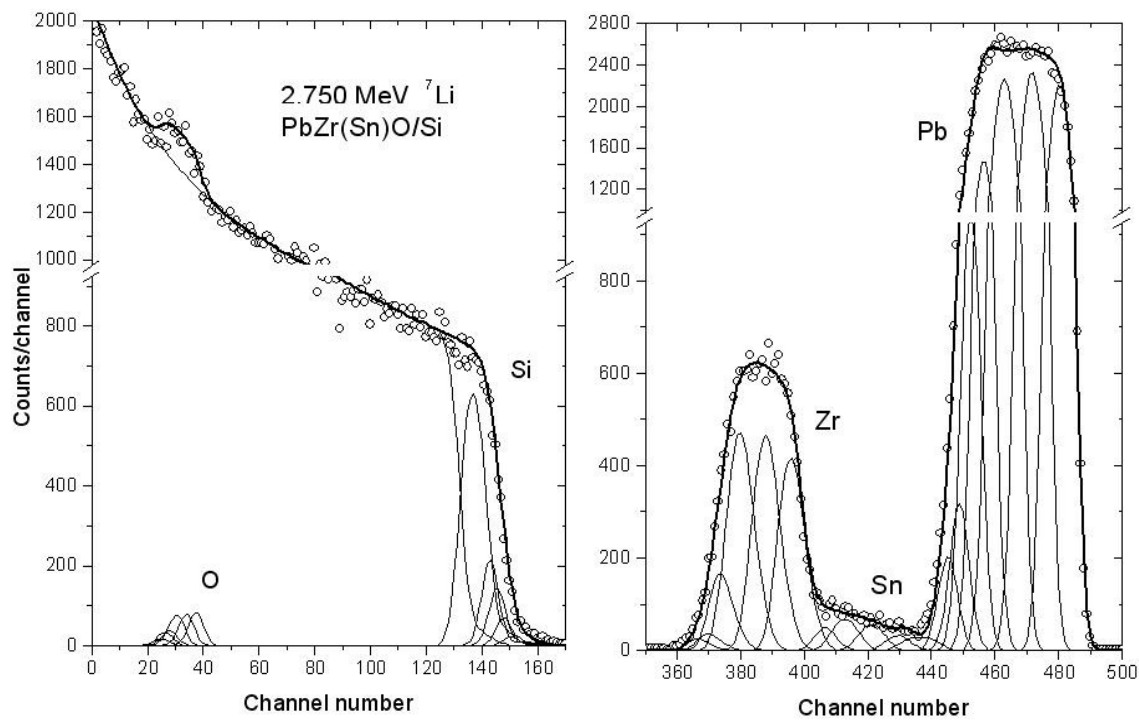
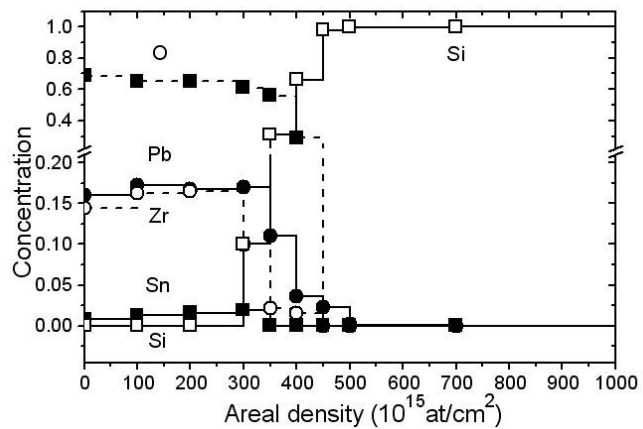


Fig. DA2. Backscattering spectrum for 2.75 MeV ^7Li ions incident on a PbZrSnO thin-film sample on a Si substrate. The thick solid line connecting the experimental data points is the simulated spectrum.

Fig. DA3. The constant concentrations of the elements (see table below) versus areal density. **Table** of experimental parameters and concentrations of the elements and the areal densities of the sublayers.



Incident particle ${}^7\text{Li}$
 $E_0 = 2750 \text{ keV}$
 $\delta E = 4.424 \text{ keV/ch}$
 $Q\Omega = 9.687 \text{ } \mu\text{C msr}$
Scattering angle 165°
Angle of incidence 60°
Exit angle 45°
System resolution 25 keV FWHM

Sublayer	10^{15} at/cm^2	Pb	Sn	Zr	Si	O
1	100	0,16	0,0075	0,145	0	0,6875
2	100	0,173	0,0128	0,163	0	0,6512
3	100	0,168	0,0155	0,165	0	0,6515
4	50	0,17	0,019	0,1	0,1	0,611
5	50	0,11	0	0,022	0,31	0,558
6	50	0,036	0	0,0153	0,66	0,2887
7	50	0,023	0	0	0,977	0
8	200	0,0015	0	0	0,9985	0
9	5000	0	0	0	1	0

None of the layers are assumed to contain any undetected light elements. The oxygen signal was not fitted, the oxygen concentration follows from the concentrations of the heavier elements, it is presumed to make up the total concentration of each sublayer to 1. Bohr straggling and a scaled stopping of $1.08 \times \text{TRIM-91}$ stopping were assumed for the metal oxide layers.

The example is intended to demonstrate how the composition variations may be treated as constant composition sublayers. As discussed in section 3.4.6 the interdiffusion and interfacial roughness can usually not be distinguished by using a backscattering spectrometry. In the present case, the probable cause for the mixing of the elements at the interface is diffusion, since the atomic layer deposition of the metal oxide film should not change the smooth Si surface.

2.3 Interactive vs. automated

The iterative procedure can be made in an interactive way, where the user repeatedly refines the depth profile until it is considered that better agreement cannot be reached within the time and patience limits of the user; or with an automated process based on optimization of some target function such as a χ^2 or likelihood function.

Caution is needed when using automated optimization. Different depth profiles can lead to the same simulated spectrum (Butler, 1990), and the code has no way of knowing which of the possible solutions is the correct one. The user must often restrict the solution space, for instance by making only a local optimization on a limited number of parameters, one at a time.

A second problem is that the χ^2 function is very sensitive to the quality of the simulation: for instance if straggling is not included, an automated procedure will return interfacial mixing layers that may not exist. This can be solved naturally by including straggling, but there are some physical effects for which no accurate analytical simulations have been developed so far. In such cases, fully automated processes will lead to artefacts in the depth profiles derived, unless the user restricts the solution space to physical solutions.

In any case, some form of automation is desirable, particularly if large quantities of data are to be analyzed.

2.4 Deterministic vs. Stochastic (Monte Carlo)

Deterministic codes follow a calculational procedure defined a priori. In simulations, the sample is divided into thin sub-layers. The incoming beam energy, as well as the detected energy for scattering on each element present, are calculated for each sub-layer. The simulation is then constructed based on these quantities and on the concentration of each element in each sub-layer. Straggling and other physical phenomena may be included. However, individual collisions between the analyzing ion (and its electrons) and the target nuclei and electrons are not modeled.

These deterministic simulations are normally very fast, lending themselves very well to the interactive and automated procedures described above, and are in fact the standard way of doing things.

Monte Carlo codes work in a completely different, more fundamental, way. They model individual interactions between particles. In this way, phenomena that have been traditionally difficult to include in the standard method, are included in a natural way. The quality of the simulations that can be reached is, in principle, much superior.

However, there are issues with the calculation times required. Even with modern computers, acceleration techniques to speed up the calculations must be used. These include for instance disregarding collisions with scattering angles smaller or larger than values defined a priori, increasing artificially the scattering cross section or the solid angle of the detector in order to have more events. This can affect in some cases the quality of the simulations.

A second issue is related to the fact that Monte Carlo codes often require very detailed knowledge about the physics involved, and so far, their usage has remained mostly confined to the code authors. Until recently almost all data analysis was made using deterministic codes (the largest exception was the use of Monte Carlo codes for the analysis of channeling data).

Nevertheless, improvement of the calculation times, coupled with development of user friendly interfaces, means that Monte Carlo codes are becoming more widespread, and may become dominant in areas such as heavy ion ERDA, where multiple scattering and special detecting systems play a large role.

3. Capabilities of codes

In this section, we discuss some of the considerations that are important when selecting a code. We note that there is no such thing as a “best code” for all situations. All codes that we know do well what they were designed to do, as a recent intercomparison exercise organized by the International Atomic Energy Agency (IAEA) showed (Barradas et al., 2007c). No code is complete in the sense that it can analyze all possible IBA data.

The codes that took part in the IAEA intercomparison exercise have been compared numerically and validated. Some of their most important characteristics are shown in **Tables 1 – 7**. Characteristics of several other codes were given in ref. (Rauhala et al., 2006). We

stress that all information given is valid at the time of writing, as several codes are being actively developed.

When choosing which code to use, the users must consider whether a given code is capable to extract the information required, and how easy it is to do so with each code. A complex sample where interface roughness and multiple scattering play a crucial role may need a last generation code, but to determine the thickness of a thin film with one single heavy element on a light substrate a full Monte Carlo calculation is probably too much work without extra benefit. Also, in some cases manual calculations with careful consideration of error sources may be the most accurate method (see for instance Boudreault et al., 2002).

3.1 Design basis

The first consideration is obviously whether the data to be analyzed are within the design basis of the code considered. The two main points are the techniques implemented by each code and, for each technique, the experimental conditions supported.

For instance, if a code can only analyze RBS data with H and He beams, there is no point in trying to use it to analyze NRA data, but it may be a possible to adapt it to analyze RBS with heavier ions, particularly if the source code is available.

In a similar way, even if a code includes e.g. RBS, it may be limited to given experimental conditions. One example is the detection geometry - some codes include not only the well-known IBM and Cornell geometries, but also general geometry where any location of the detector is allowed (including transmission). Another one is the detection system, with most codes including only energy-dispersive systems, while some can include velocity and time of flight spectra, magnetic spectrometers, and others.

3.1.1 Techniques implemented

As stated above, this chapter is aimed predominantly at RBS and ERDA software packages. EBS is in practice RBS with non-Rutherford cross sections that must be given by the user (or included in the code) for each given ion/target nucleus pair.

Non-resonant NRA is also included here because it also uses one single beam energy (as opposed to resonant NRA, where the energy is scanned), and it is common that both the scattered beam and some reaction product are detected simultaneously.

Techniques such as channeling, PIXE, or resonant NRA, are included in some of the codes.

Table 5 shows the techniques implemented in each code. All implement RBS, but some do not include ERDA or NRA. NDF is the only one to include PIXE. Note however, that some labs only do RBS, and it may be convenient to use a code with fewer options (thus possibly easier to use) that can do what the user needs and nothing else. However, most labs have several techniques available, and using the same code to analyze all the data has obvious advantages.

3.1.2 Experimental conditions supported

Table 5 shows also the experimental conditions that each code supports. They are similar in all codes, which handle most situations. Some differences exist, and users who need special conditions should consider carefully the capabilities of the codes. Also, it may be possible to convince authors of codes still under development to implement some specific experimental condition not previously covered. If the source code is available, expert users can modify them according to their convenience.

3.1.3 Description of samples

One of the most important points in codes is how conveniently the sample can be described. This is illustrated in **Table 7**.

Homogeneous layers are considered in all codes that participated in the IAEA intercomparison exercise, and in almost all codes known to us. In some codes, functions describing continuous profiles can also be introduced, which is important if for instance diffusion of implant profiles are being analyzed.

Sometimes a maximum number of layers or of elements in a given layer is imposed. When restrictions on the number of layers exist, problems can arise when a very thin layer description is required. This is the case if the sample has many thin layers, or in high-resolution experiments (for instance using a magnetic spectrometer or grazing angle geometry).

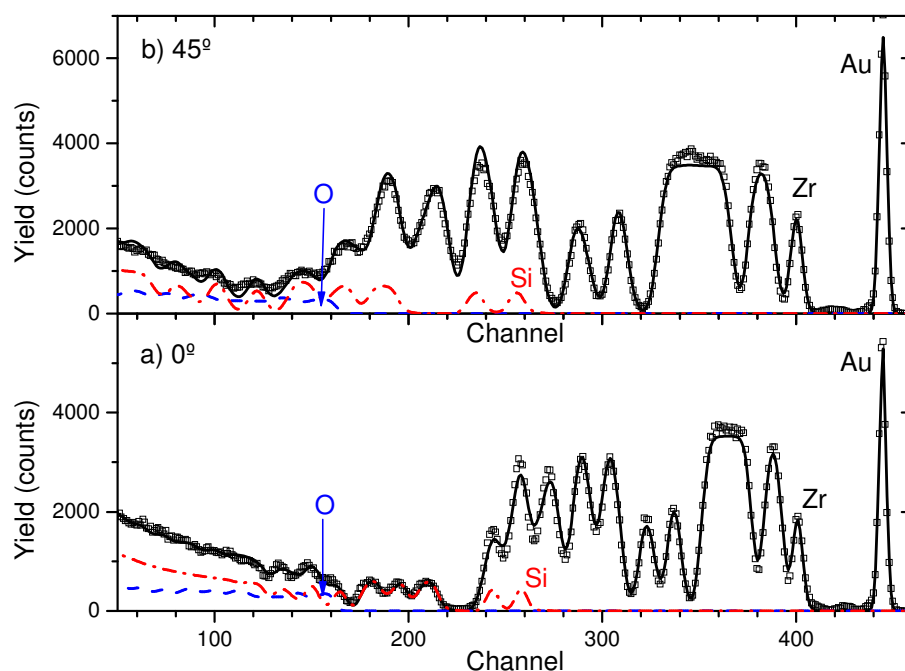


Fig DA4. Data and fit (solid line) obtained for a 21-layer antireflection ($\text{ZrO}_2/\text{SiO}_2$) antireflection coating with a top Au layer, shown for the data collected at: (a) normal incidence; (b) 45° . The fitted partial spectra for Si and O are also shown.

RBS spectra are ambiguous whenever more elements are present than spectra were collected (Butler, 1990, and Alkemade et al., 1990). That is, more than one different depth profile can lead to exactly the same simulated spectrum. To remove ambiguities, more spectra should be collected, with different experimental conditions. However, often the elements are bound in molecules, allowing the analyst to connect the respective signals to each other; for instance, if SiO_2 is present, the small O signal can be connected to the much larger Si signal by imposing the known stoichiometry. One very useful function in a code is therefore to allow the user to use as logical fitting elements not only atomic species, but molecules as well. The molecules can be of known or unknown composition. In the latter case, such a code would fit the molecular stoichiometry together with its concentration in each layer. One example is shown

in the Pitfalls chapter of this Handbook.

We show in **Fig. DA4** the RBS spectra of a 21-layer ($\text{ZrO}_2/\text{SiO}_2$) antireflection coating with a top Au layer (Jeynes et al., 2000a). The Zr had a small (known) Hf contamination. Both normal incidence and a 45° angle of incidence were used. The O, Si and Hf signals are small and superimposed to the much larger Zr signal. It is virtually impossible to meaningfully analyze these data without introducing the chemical information in some way. The two spectra were fitted simultaneously, imposing as logical fitting elements the known molecules. The small $\approx 5\%$ misfits can be due to inaccurate stopping or small deviations from stoichiometry. In any case, complete disambiguation of the data is achieved.

3.2 Data bases implemented

One of the main conclusions of the IAEA intercomparison exercise of IBA softwares was that the largest differences in the results arise from differences in the fundamental data bases used, namely the stopping power data base, but also the non-Rutherford data base in the case of EBS, ERDA, and NRA.

In the last decade important advances have been made both in terms of new and more accurate experimental data, and in new theoretical and semi-empirical schemes. Which data bases are included in each code, as well as the possibility of loading in new values, is thus an important factor.

3.2.1 Stopping power

The largest changes in the knowledge of stopping power registered in the last decade were for heavy ions. This was possible due to a wealth of new experimental data becoming available, which was integrated for instance in the most widely used stopping power semi-empirical interpolating scheme used in IBA work, SRIM (Ziegler, 2004, Ziegler et al., 2008), but also for instance in MSTAR (Paul and Schinner, 2001, and Paul and Schinner, 2002), which is dedicated to heavy ions. See the Chapter on Energy Loss.

For instance, we show in **Fig. DA5** the calculated spectrum for 3 MeV ^7Li beam incident normally on a Si/SiO_2 2×10^{18} at./cm²/Ti 1.5×10^{18} at./cm² sample and detected at 160° , using 1985 stopping power values and SRIM version 2006.02. It is clear that the very large changes in the simulation will be reflected in the accuracy of analyses of real data, with errors up to 10% being made in thickness values, depending on the stopping values used.

Large changes also occurred for light ions in some common systems. For instance, the stopping of He in Si is now known with an accuracy better than 2%, which has been integrated in SRIM and other data bases.

Also, many experiments in insulating compounds have shown that the Bragg rule does not always reproduce the experimental stopping, and the capability of including molecular stopping powers in codes is very important.

The stopping power along crystalline directions is usually smaller than in a random direction or in an amorphous material with the same composition.

Ideally, codes should include the most recent stopping power databases available, and also the possibility of loading in new stopping values for particular systems. In any case, the users of data analysis software must be aware of the stopping used in a given analysis, and its implications for the accuracy of the results obtained.

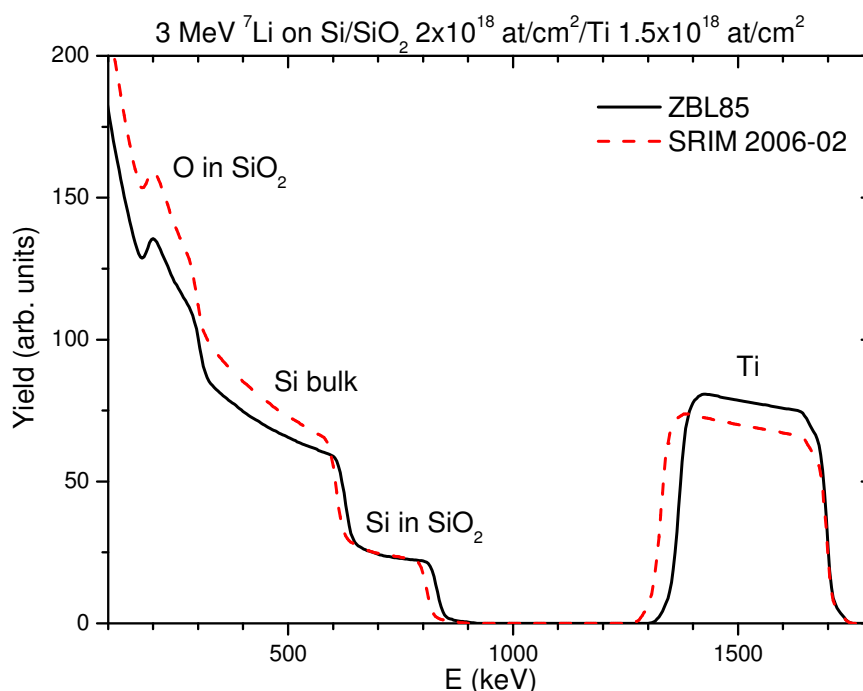


Fig. DA5. Calculated spectra for 3 MeV ^7Li beam incident on a Si/SiO₂ sample. The only difference between the simulations is that different stopping powers have been used: from 1985, and the most recent available ones. Users of data analysis codes must be aware of the stopping used by the codes.

3.2.2 Scattering cross section

When analyzing EBS or NRA data, and also for instance ^4He -ERDA measurements of hydrogen isotopes, the non-Rutherford cross section used is of paramount importance. Some codes include a wide data base of cross section values for given ion/target pairs, while others read in external data files with the cross section required.

The code SigmaCalc (Gurbich, 1997, Gurbich, 1998, and Gurbich, 2005) for calculating the cross sections from tabulated theoretical model parameters was developed by A. Gurbich. SigmaCalc is usually very reliable for those ion/target pairs that it includes, and allows one to interpolate for scattering angles for which no measured cross section is available. This action has also led to the integration of NRABASE and SIGMABASE into a single database called IBANDL, under the auspices of the IAEA.

Data with slowly changing non-Rutherford cross sections can be analyzed manually, as shown for instance in Chapter 4 of the 1st Edition of the Handbook of Modern IBA (Tesmer and Nastasi (eds), 1995) for ^4He -ERDA analysis of hydrogen in Si₃N₄(H). However, this is a painstaking procedure that can be done much faster, and more accurately, by computer simulation.

When superimposed signals with fast changing cross-sections are present, then it becomes almost impossible to analyze the data manually, and computer codes must be used, using the appropriate cross sections. We show in **Fig. DA6** 1.75 MeV ^1H backscattering off a TaNiC film on Si (Jeynes et al., 2000b). The C signal is superimposed on the Si background, and both signals change rapidly due to the presence of resonances in both cross sections. The simulation includes one single homogeneous TaNiC layer, and is the result of an automated

fit that took less than 1 minute. The scattering cross sections for C and Si were taken from SigmaCalc, and for Ta and Ni they are screened Rutherford.

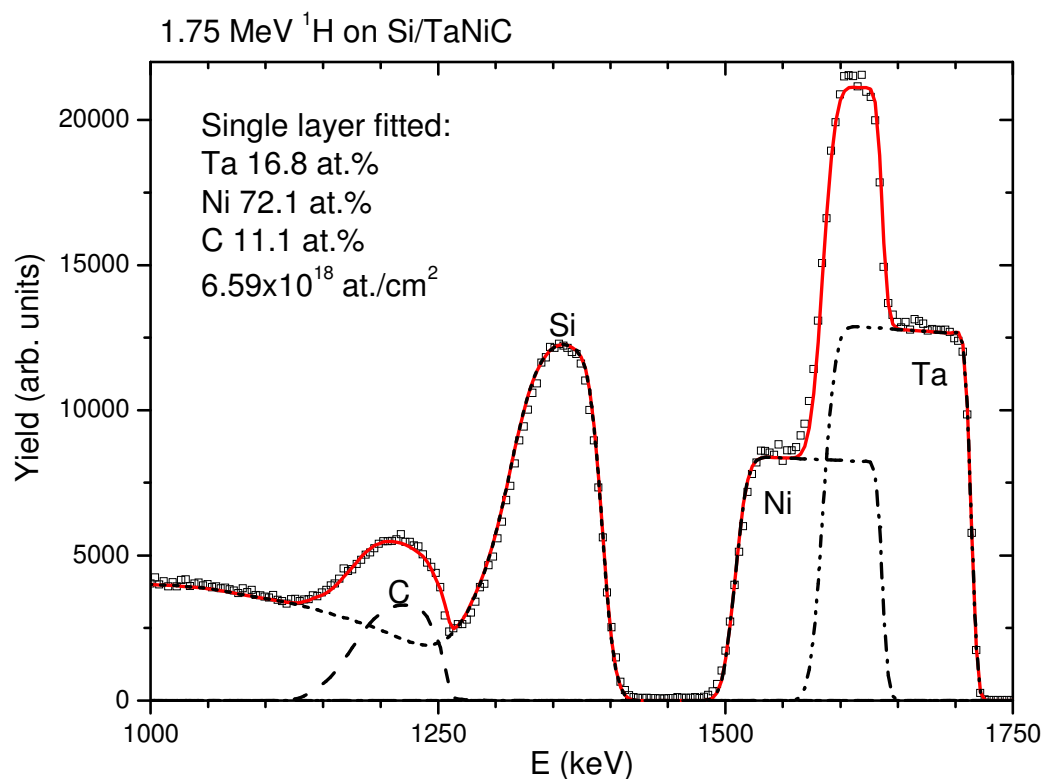


Fig. DA6. Spectrum for 1.75 MeV ^1H backscattering off a TaNiC film on Si.

3.3 Basic physics

All codes (except the Monte Carlo ones) adopt similar principles to make a basic simulation. The ingoing beam follows a straight trajectory, while losing energy; it interacts with a target nucleus; and the outgoing beam follows a straight trajectory, while losing energy, on its way to the detector. The energy spread of the beam (often called straggling) is also calculated.

From the point of view of the user, the fact that the different codes implement these things in very different ways is not important.

The user wants to know, first, that all codes make good simulations (at least for simple everyday spectra; complex samples may require particular codes). Proving that a code is correct would imply a deep analysis of the physics included and of its implementation into algorithms. Users do not want to do this, and often can't (either because the source code is not available, or because they don't have the time or the necessary background). Until recently, users simply assumed that codes are correct.

The IAEA intercomparison exercise showed that all codes produce similar results for a 1.5 MeV ^4He RBS simulation of a simple sample. Signal total yields and signal heights are calculated with a 0.1 to 0.2% standard deviation between codes (as long as the same stopping powers and scattering cross sections are used by all codes). This is thus the error due to the differences in implementation of the same physics. It is smaller than the usual experimental

errors coming e.g. from counting statistics (rarely better than 1%), and much better than the error in the stopping power values.

With the assurance that the codes (at least those that participated in the IAEA intercomparison) are correct for simple cases, the user may be concerned with how fast the simulations are. With modern computers, simulation of simple spectra, even with straggling included, is always fast. Efficiency only becomes important when some further physics, such as plural scattering, is included.

3.4 Advanced physics

While all simulation codes treat basic ion stopping and scattering phenomena, many of the subtle features in spectra arise from more complex interactions. The main issues involve energy spread, multiple and plural scattering, the handling of non-Rutherford cross sections, surface and interface roughness, and channeling.

The first comment is that, in principle, the best way of dealing with all of these is full Monte Carlo simulations. MCERD, for instance, is a code for analysis of ERDA data, but it can also handle RBS. It can include all of these effects, except for channeling. Different codes have been dedicated to the analysis of channeling of specific systems.

However, MC codes are mostly used by their authors, and calculation times can be an issue. Development of intuitive user interfaces, and continuing gains in efficiency may change this situation, but for the moment traditional codes are still the most used. What follows is therefore related to traditional codes

We are concerned with knowing in which situations the basic simulations discussed in section 3.3 are adequate. In situations where they are not adequate, we want to know whether codes include enough further physics to lead to meaningful analysis. The capabilities of the different codes are summarized in **Table 6**.

3.4.1 Straggling models

Practically all codes implement the Bohr model (Bohr, 1948); with or without the Chu/Yang correction (Chu, 1976, and Yang et al., 1991), important for He and heavier beams; and some implement the Tschalär effect (Tschalär, 1968, and Tschalär and Maccabee, 1970), which can be important in thick layers (for instance to calculate the energy spread in a buried layer, or after a stopper foil). Some codes let the user scale the calculated straggling. We note that pure Bohr straggling (without the Tschalär effect) is valid in a rather narrow range of energy loss, typically when the energy loss does not exceed around 20% of the initial beam energy.

However, straggling is only important if the detailed signal shape carries relevant information. To determine the stoichiometry and thickness of films, it is very often irrelevant, and the user can either ignore it, or adjust the straggling to match observed signal widths. In this case, all codes will do fine.

If, on the other hand, interdiffusion or roughness between layers are being studied, or if a changing depth profile must be derived with maximum achievable accuracy, then any error in the straggling will directly lead to an error in the results. In such situations, best available theory (i.e., a code that implements it) must be used.

State of the art calculations of straggling, including geometrical straggling and multiple scattering, are made by the code DEPTH (Szilágyi et al., 1995, Szilágyi, 2000).

No code dedicated to general purpose IBA data analysis implements accurate straggling functions such as the Landau-Vavilov function. See for instance Bichsel, 2007 and references therein for a detailed discussion.

3.4.2 Electron screening

Electron screening at low energies decreases the effective charge of the target nucleus seen by the analyzing ion, leading to a smaller scattering cross section (L'Ecuyer et al., 1979, and Andersen et al., 1980). It is larger for heavier target species and heavier ions, and for lower energies. For 1.5 MeV ^4He RBS off gold, it leads to a 2% correction to the cross section. Most codes implement this.

3.4.3 Plural scattering

Plural scattering involves a few large-angle scattering events. It leads to a low energy background, to an increased yield of bulk signals at low energies, and it can lead to yield above the surface energy. It can normally be disregarded, even when it is sizeable, because it changes slowly with energy, and ad-hoc backgrounds or signal subtraction techniques are often used.

It is important in the rare occasions where the yield at low energies or in a given background region must be understood quantitatively. Also, at grazing angle (of incidence or detection) it can be a large contribution even to the signal of fairly thin surface films. SIMNRA (Eckstein and Mayer, 1999) and NDF (Barradas, 2004) can calculate double scattering (two large angle events, which accounts for most plural scattering). The two algorithms are not equivalent but lead to similar results in most situations. In some cases, such as in grazing angle geometry, large differences may exist, and the user should study the respective literature. Calculations are slow and not as accurate as for single scattering, but excellent reproduction of observed signals can be obtained, as seen in **Fig. DA7** (Mayer, 2002).

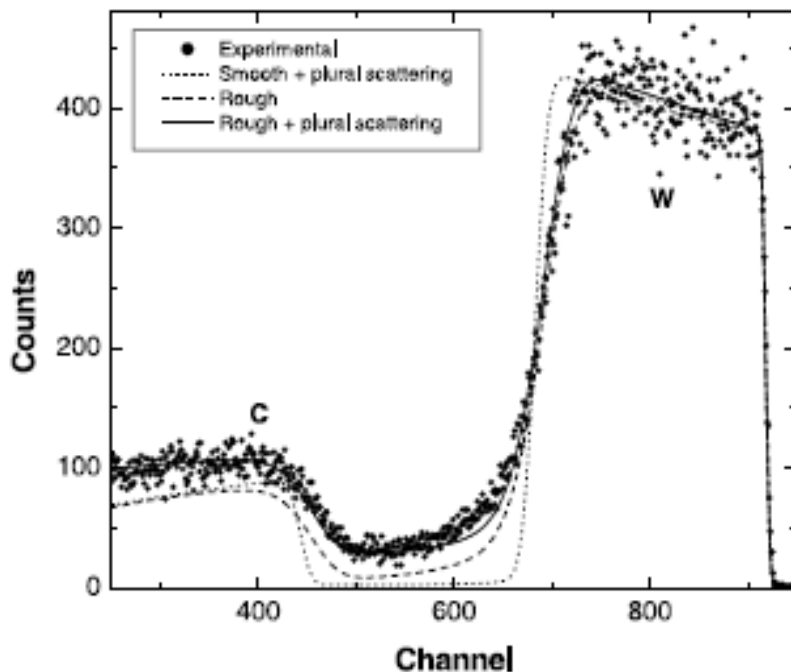


Fig. DA7. 2.5 MeV p backscattered from 3.5 μm W on a rough carbon substrate, normal incidence, scattering angle 165° . (dots) Experimental data; (dotted line) calculated spectrum for a smooth W layer (3.6 μm) on a smooth C substrate including plural scattering; (dashed line) calculated spectrum for a rough W layer (3.5 μm , $\sigma = 0.30 \mu\text{m}$) on a rough substrate (FWHM 20°); (solid line) as dashed line, but including plural scattering (From Mayer, 2002).

3.4.4 Multiple scattering

Multiple scattering involves a large number of low-angle scattering events. It changes the trajectories of the beam ions, making them quite different from straight lines. This has many consequences, some of which standard codes are unable to calculate. We want to know when it is important, and when can we calculate its effects well enough.

Multiple scattering leads to an extra contribution to the energy spread of the beam; to a change in the shape of signals because this contribution is not Gaussian-shaped; and to a change in observed yield.

It is more important for heavier ions at lower energies in heavier targets, and for grazing angles. In fact, at near-normal incidence and detection of ions with energies in the usual IBA range, it can almost always be ignored.

At grazing angle (for instance in ERDA), multiple scattering is often the most important contribution to energy spread. If energy spread is important (see section 3.4.1), then it must be calculated.

The best available calculations of multiple scattering (but not necessarily the best simulation of energy spectra) are made by the code DEPTH (Szilágyi et al., 1995). Some codes implement the extra energy spread, but assume it to be Gaussian-shaped. Most codes do not calculate multiple scattering. For heavy ions at fairly low velocities in grazing angle geometry, none of the standard codes compares very well with Monte Carlo calculations, at the time of writing.

3.4.5 Simulation of resonances

It is quite difficult to simulate buried sharp resonances. “Buried” and “sharp” means whenever the energy spread of the beam before scattering is comparable to the resonance width. For bulk signals, the shape of the resonance signal is considerably affected; for thin films, the actual yield is also affected. This is important whenever a sharp resonance is used to enhance the yield from a buried element.

For instance, for protons crossing a 4.2 μm Ni film (leading to a high energy spread) on top of a 1 μm Mylar film, the calculated C yield from the Mylar can be a factor of 10 wrong if the energy spread of the beam is not taken into account (see fig. 10 of Barradas et al., 2006).

As far as we know, the only code for analysis of general RBS and ERDA data that is currently able to calculate correctly the shape and yield in the presence of buried sharp resonances is NDF (Barradas et al., 2006). Dedicated codes for specific systems (Tosaki et al., 2000) and for resonant NRA (Vickridge et al., 1990, Pezzi et al., 2005) also exist.

3.4.6 Surface and interface roughness

There is no general definition of roughness. Many different types of roughness exist. In the context of IBA, the most important point is that, in general, RBS experiments are not enough to determine which type of roughness is present. In fact, they are not even enough to distinguish between layer interdiffusion and interfacial roughness. In almost all cases, extra information from other techniques (usually TEM or AFM) is required. That said, RBS can be very useful to quantify roughness in some cases.

Several methods exist to simulate spectra including roughness. The most accurate is to make a Monte Carlo simulation, modeling the desired surface or interface. This is not amenable to routine data analysis.

A usual approach in analytic codes is the summation of partial spectra over a distribution function of some sample characteristics, such as surface height, film thickness, or other. RUMP and SIMNRA implement different variations of this method.

A second approach is to calculate analytically the effect on signal width due to a given type of roughness, and take it as an extra contribution to energy spread. Spectra can be calculated in the usual way. NDF implements this method, which has stringent but well defined conditions of applicability, for 5 different types of roughness, and also for inclusions, voids, and quantum dots. Both approaches ignore correlation effects and fail for features with large aspect ratios leading to re-entrant beams.

An analysis done with SIMNRA of a rough sample is shown in **Fig. DA7** (Mayer, 2002), where plural scattering also plays an important role. The sample is a rough W layer on a rough C substrate, which is a very complex situation. Quantitative information on the roughness parameters is obtained in a relatively simple way, as the user only needs to specify the roughness type and amount, and the code takes care of all the calculations.

3.4.7 Channeling

Specific methods have been developed to analyze channeling data. Most standard analytic codes are simply not capable to analyze channeling. Some implement ad-hoc corrections to the channeled yield in order to be able to derive information from unchanneled parts of the spectrum. Only one of the standard codes that participated in the IAEA intercomparison exercise, RBX, is actually capable of simulating the channeled RBS spectra of virgin crystals and even with point defect distributions.

3.4.8 Pulse pile-up

Pile-up leads some counts being lost and some counts being gained in the spectrum collected. Without exception, more counts are lost than gained, and so the total yield, integrated over the entire energy range, is smaller than it would be for a perfect detection system.

Some codes calculate pile-up based on system parameters such as amplifier type, shaping time of the amplifier, beam current, collection time, and characteristic time of a pile-up rejection circuit if present (Wielopolski and Gardner, 1976, Gardner and Wielopolski, 1977, and Wielopolski and Gardner, 1977). This can be important in some cases, particularly given that pile-up is not linear, and can be a correction of several % to the yield. It should be calculated always, except for very low count rates. The chapter on Pitfalls shows an example.

3.5 Automated optimization

Practically all codes can work interactively. The user looks at the data, makes an initial guess of the sample structure, calculates the corresponding theoretical spectrum, and compares it to the data. Differences drive modifications in the structure defined until the user considers agreement is good enough (or, rather often, until patience runs out).

In automated optimization, it is the computer code that controls this procedure. Users should be aware that an objective criterion of goodness of fit is needed, usually a χ^2 or likelihood function. It is this function that the codes try to optimize. This can lead to a serious pitfall. If the model does not describe all the relevant physics (for instance if multiple scattering is important but not calculated, or poorly calculated), or if the user introduced too little or too many elements in the sample description, a good fit that also corresponds to the true sample structure cannot be obtained. The code will output something, but this will not be a good

solution. We cannot overemphasize the fact that automated optimization is a wonderful feature, but it can lead to large errors unless great care is taken in checking the results.

If several spectra were collected, the possibility of fitting them all simultaneously, with the same sample structure, is essential to ensure consistency of the results and that all the information present in the spectra is taken into account to generate the final result.

3.5.1 Fitting

Automated fitting is designed to relieve the user from this task. Not all codes do it. Some, such as RUMP and SIMNRA, do a local optimization on a limited number of parameters, starting from an initial guess, which usually must include the correct number of layers.

NDF uses an advanced algorithm, simulated annealing (Kirkpatrick et al., 1983), complemented by a local search, to find an optimum solution without any need for initial guess, except for the elements present. All parameters can be fitted.

3.5.2 Bayesian inference

IBA is often fully quantitative without needing standards. This is arguably its greatest strength. However, actual error bars or confidence limits on the concentration, thickness values, or depth profiles determined are almost never presented or published. This is arguably the greatest weakness of IBA work.

In the last decade, Bayesian inference (BI) methods have been applied to IBA data analysis, providing a tool to systematically determine confidence limits on the results obtained (Barradas et al, 1999, Padayachee et al., 2001, Neumaier et al., 2001, Mayer et al., 2005, and Edelmann et al., 2005). The mathematics is somewhat involved, but the users of codes do not need to be concerned with it.

In practical terms, instead of producing one best fit, for instance minimizing the χ^2 , BI makes a series of simulations, for very many different samples structures and depth profiles, all of them consistent with the data. Moments, such as the average and standard deviation, can then be calculated.

During the BI calculation, the known experimental errors can be introduced. The error in the energy calibration, solid angle, beam fluence, and even beam energy or scattering angle can be introduced. These errors, together with the statistical counting error, will be reflected in the final error calculated for the depth profile.

MCERD and NDF both implement BI. It is computationally expensive, that is, it takes much longer to make a BI run than to make a least-squares fit. For the moment, BI is still not suitable to routine analysis of large amounts of data. A few samples per day can however be analyzed, and BI is the only method that can deliver reliable error bars in a general way.

3.6 Usability and usage

Usability of a code refers to how easy it is to use the code correctly. This depends on how intuitive and simple the user interface is, but also on how much knowledge the user has about the technique used. Non-expert users may not know that scaling a given stopping power by a factor of 2 may not be justifiable, or that intermixing and surface roughness can have the same effect on measured data. Many other examples can be easily found by reading carefully published work, where inaccurate or wrong results due to bad data analysis are unfortunately not uncommon.

The easiest code to use is often considered to be RUMP, whether in its command-line or windowed incarnations, and no chapter on IBA software could go without citing its “beam me

up Scotty” command line. First generation codes such as GISA already had strong graphical capabilities and easy to navigate menus. RBX allows quick editing of parameters for analysis of multiple spectra.

The new generation codes have more user options and as a consequence are perhaps not as intuitive. To use advanced physics features often requires knowledge of the issues involved and of an increased number of system parameters. As a consequence, usage (particularly by novices) is more prone to errors. SIMNRA is considered easier to use than NDF. Their manuals state they are “easy to use” (Mayer, 2007) and “designed for experienced analysts of Ion Beam Analysis data” (NDF, 2007), respectively. MC codes such as MCERD are not yet widely used except by the authors and their collaborators.

The IAEA intercomparison exercise originally planned to test usability by novices and expert users, but this has not yet been done.

RUMP is historically the most cited IBA data analysis code, with around 120-150 citations per year in the last decade. SIMNRA came a close second in 2007, and if the trend continues, it will overtake RUMP as this book is published. NDF, the third most cited code, receives about half the citations that SIMNRA does. SIMNRA and NDF combined now account for more citations than RUMP does. Citations may be misleading when trying to assess real usage of a code, since users may not always cite the code they use.

4. Accuracy

The accuracy that can be achieved in an IBA experiment depends on many parameters. For each given experiment, an uncertainty budget can be made, including all the different sources of error. A detailed example is discussed in the Pitfalls in Ion Beam Analysis chapter of this Handbook.

Data analysis codes cannot lead to results that are more accurate than the models applied and experimental data analyzed. Furthermore, most of the codes usually do not produce an error analysis, just numbers without associated accuracies. The consequence is that it is almost universal practice to quote the results provided by the codes, such as concentrations, layer thicknesses, or depth profiles, without quoting the associated uncertainties. Given that IBA techniques such as RBS or ERDA are inherently quantitative, this is not really justifiable.

Bayesian inference can be used to make an error analysis (Barradas et al., 1999), but it is not implemented in most codes, and it is computationally intensive. The uncertainty budget is a valid alternative, but it requires detailed knowledge that many users do not have.

4.1 Numerical accuracy of codes

The codes themselves have an associated accuracy. For exactly the same sample structure and experimental conditions, and including exactly the same physics, no two codes will calculate numerically the same theoretical spectrum. Differences in implementations of the physics, algorithms, and even in floating point representation do lead to differences in the calculated spectra, and thus to different final results of the data analysis. The question is, how large are these differences.

The codes that took part in the IAEA intercomparison exercise (Barradas et al., 2007) have been compared numerically and validated. For ^4He RBS, differences up to 0.2% were found. For ^7Li RBS, this increased to 0.7%. For ^4He ERDA, differences between 0.5 and 1.3% were found in calculated yield values. This is a further source of inaccuracy that should be included in the uncertainty budget. We note that experimental uncertainties down to about 0.5% are difficult to reach, but have been reported (Jeynes et al., 2006, Barradas et al., 2007). This

means that at least for ERDA and heavy ion RBS, the accuracy of the calculations can be an issue.

However, if we consider only the codes RUMP, NDF and SIMNRA, which together account for over 80% of citations in work published in 2006 and 2007, then the differences are 0.1% for ^4He RBS, 0.3% for ^7Li RBS, and 0.1% for ^4He ERDA. This is significantly better than achievable experimental uncertainty, and much better than the uncertainty with which stopping powers are currently known.

4.2 Intrinsic accuracy of IBA experiments

The intrinsic accuracy of IBA experiments is limited by three main factors: the accuracy of the models applied and how well the related basic physical quantities such as cross sections or stopping powers are known; the accuracy with which the experimental parameters are known; and the counting statistics.

4.2.1 Models and basic physical quantities

Many different models are used in IBA data analysis to describe the various physical phenomena involved. The accuracy of these models is often difficult to assess. Examples are stopping and scattering cross sections, plural and multiple scattering, screening, the energy spread, the detector response, pileup, etc. A few examples are briefly considered below.

The accuracy of scattering cross sections is limited at high energies by the occurrence of elastic nuclear reactions. In this case, experimental or cross sections evaluated by using nuclear models must be used (see e.g., IBANDL). The errors involved depend on the error of the cross section measurements. Users interested in accuracy must check the original literature for each reaction, but accuracies better than 1-2% are almost never achieved, and 10% is common. Given that many cross sections have a strong angular dependence, the uncertainty in the scattering angle leads to an even larger error, which is difficult to evaluate. The nuclear models can predict scattering at angles where experimental data are not available.

In the low energy limit, electron screening becomes the issue. For 1 MeV $^4\text{He}^+$ backscattered off Ta, the cross section is already 3% smaller than the Rutherford formula (Rauhala, 1987). For 0.3 MeV $^4\text{He}^+$ forward-scattered off Au at a 15° angle, the correction is about 33% (Andersen et al., 1980). However, in both cases this can be calculated, for instance by the angular-dependent screening correction given by Andersen et al. (Andersen et al., 1980), which leads to cross sections accurate within 1% for scattering angles above 15° and $^4\text{He}^+$ energies above 0.3 keV. For the usual velocities in RBS, the accuracy is not better than 0.2% for heavy target elements such as Au.

The limited accuracy of stopping powers is a fundamental limit to the accuracy with which layer thickness and depth profiles are determined. A statistical analysis made by Ziegler shows that the average standard deviation of SRIM2003 stopping power calculations relative to experimental values is 4.2% and 4.1% for H and He ions, respectively, and 5.1% and 6.1% for Li and heavier ions, respectively (Ziegler, 2004). For H and He ions, 25% of the calculations are off by more than 5% relative to the experimental values. For heavy ions, this increases to 42% of all SRIM stopping powers, and 18% of the calculations have an error large than 10%. There are very few stopping powers known with an accuracy better than 2%. For light compounds, particularly insulators, the Bragg rule can lead to large errors (above 10% at the stopping peak).

4.2.2 Experimental conditions

The experimental conditions such as the beam energy, incidence and scattering angles, beam fluence, solid angle of the detector, MCA energy calibration, and others, all have an associated accuracy, which is often not known. The reader is referred to the Pitfalls in Ion Beam Analysis chapter of this Handbook.

4.2.3 Counting statistics

Experiments cannot last indefinitely. Often there is a limited amount of beam time allocated for a given number of samples that must all be measured. More generally, counting statistics is limited by the damage caused to the sample by the beam. In any case, Poisson statistics (often approximated as Gaussian statistics) is well understood, and is used in most error analysis actually published. One common example is to calculate the error of an isolated signal as the square root of the integrated yield. This leads to an underestimation of the true accuracy, which is often much worse than what would be granted only by statistics.

4.3 Physical effects on data analysis

The effects that some physical phenomena have on data analysis are shown in **Table 8**. Where possible, the resulting errors were quantified. Note that the error values given are indicative only and a detailed error analysis must be made in a case by case basis.

With this table in mind, the following advice can be given:

- Always include electron screening in the calculations. The angular dependence of screening is important at small scattering angles and low energies, so it should be included (in practice, Andersen et al. screening).
- For proton beams at any energy, and ^4He beams at energies as low as 2.0 MeV, always check the literature and the IBANDL for possible nuclear reactions and the corresponding cross sections.
- Always use the most recent stopping power data available. In some cases, particularly for heavy ions, this can imply using literature values and not one of the popular interpolative schemes.
- Be aware of the accuracy with which you know the experimental parameters. The nominal values cannot be taken for granted unless a strong effort has been made to determine them.

Furthermore, depending on the experiment at hand, the following points may need to be included in the analysis:

- One of the sources of the low energy background is double scattering. If an accurate low energy calculation is important, then use a code that can calculate double scattering. However, other sources, such as slit scattering, also lead to similar backgrounds and may be impossible to calculate.
- Calculate pile-up whenever the count rate is not very low, or whenever a high energy background is observed.
- All contributions to energy spread, including geometrical straggling and multiple scattering must be calculated whenever the broadness of signals is relevant to the analysis.
- Calculate the effect of surface and interface roughness whenever relevant; very often surface roughness is ignored and falsely assigned to layer intermixing.

- Read carefully sections 3.4 Advanced capabilities and 6.1 Further capabilities of this chapter, some of those may be needed to analyze your data.
- Read carefully the Pitfalls in Ion Beam Analysis chapter of this Handbook, particularly what concerns accuracy and the error budget.

5. RUMP and first generation codes

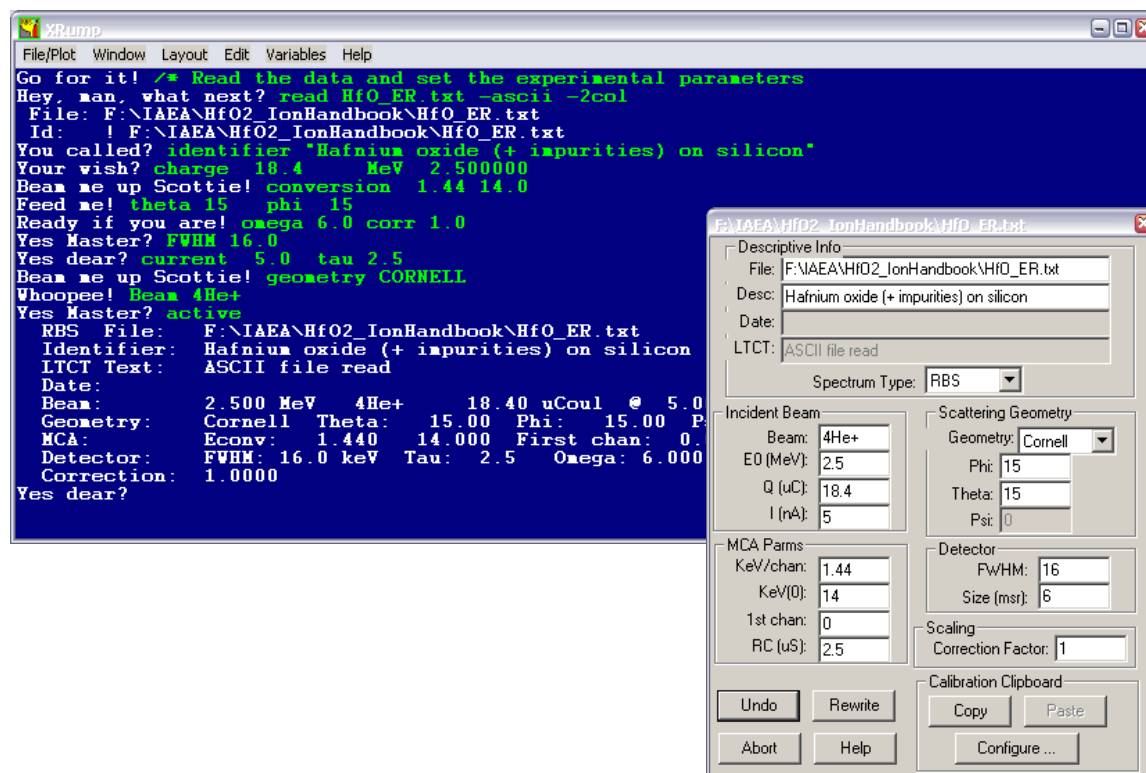
In 1976 Ziegler and co-workers published the first code, called IBA, that performed full simulations of RBS spectra. In the next decade, a series of codes surfaced, the most popular of which is RUMP (Doolittle, 1985).

There are many versions of RUMP around, including some very early ones. Users are cautioned that they should download regularly the new version (Genplot): RUMP is actively developed, and new versions incorporate for instance recent stopping powers, heavy ions, and improved algorithms.

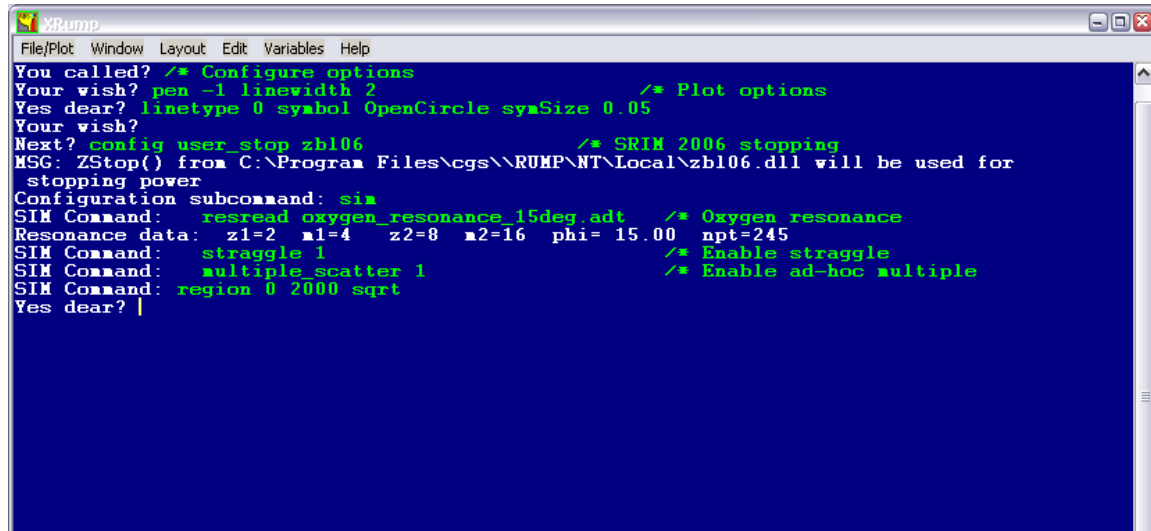
RUMP is very reliable for what it is designed to do. This, together with being easy to learn and use, is the main reason for its popularity. Novice users can obtain accurate results from simple spectra without too much work. In the RUMP **worked example DA3** we show how information can be extracted from a fairly complex spectrum by an expert user. This is one of the samples analyzed in the IAEA intercomparison exercise of IBA software.

Worked example DA3 - RUMP

The first step is to load the data and define the experimental conditions. This is made in RUMP by using an edit window or by commands given in the best known screen in IBA.



The second step can be to configure some simulation parameters using line commands. In this case, SRIM2006 stopping powers are used, the non-Rutherford scattering cross section for the $^{16}\text{O}(\alpha,\alpha)^{16}\text{O}$ is loaded, and straggling and multiple scattering are enabled. By default all isotopes are calculated separately (as opposed to making one single calculation for the average mass of the target element), and Andersen electron screening is included.

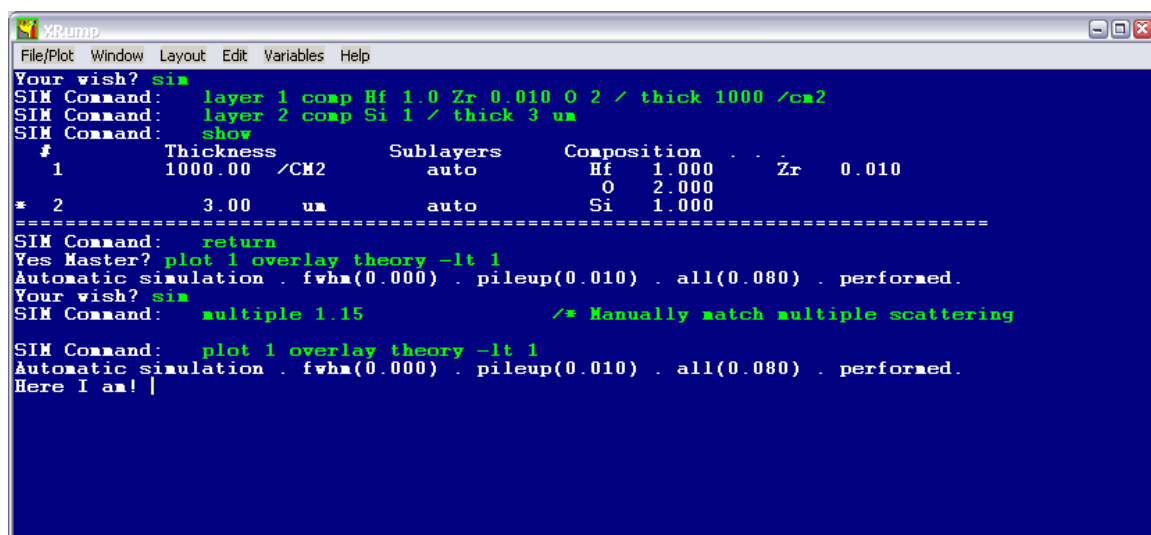


```

XRump
File/Plot Window Layout Edit Variables Help
You called? /* Configure options
Your wish? pen -1 linewidth 2 /* Plot options
Yes dear? linetype 0 symbol OpenCircle symSize 0.05
Your wish?
Next? config user_stop zbl06 /* SRIM 2006 stopping
MSG: ZStop() from C:\Program Files\cgs\RUMP\NT\Local\zbl06.dll will be used for
stopping power
Configuration subcommand: sim
SIM Command: resread oxygen_resonance_15deg.adt /* Oxygen resonance
Resonance data: z1=2 a1=4 z2=8 a2=16 phi= 15.00 npt=245
SIM Command: straggle 1 /* Enable straggle
SIM Command: multiple_scatter 1 /* Enable ad-hoc multiple
SIM Command: region 0 2000 sqrt
Yes dear? |

```

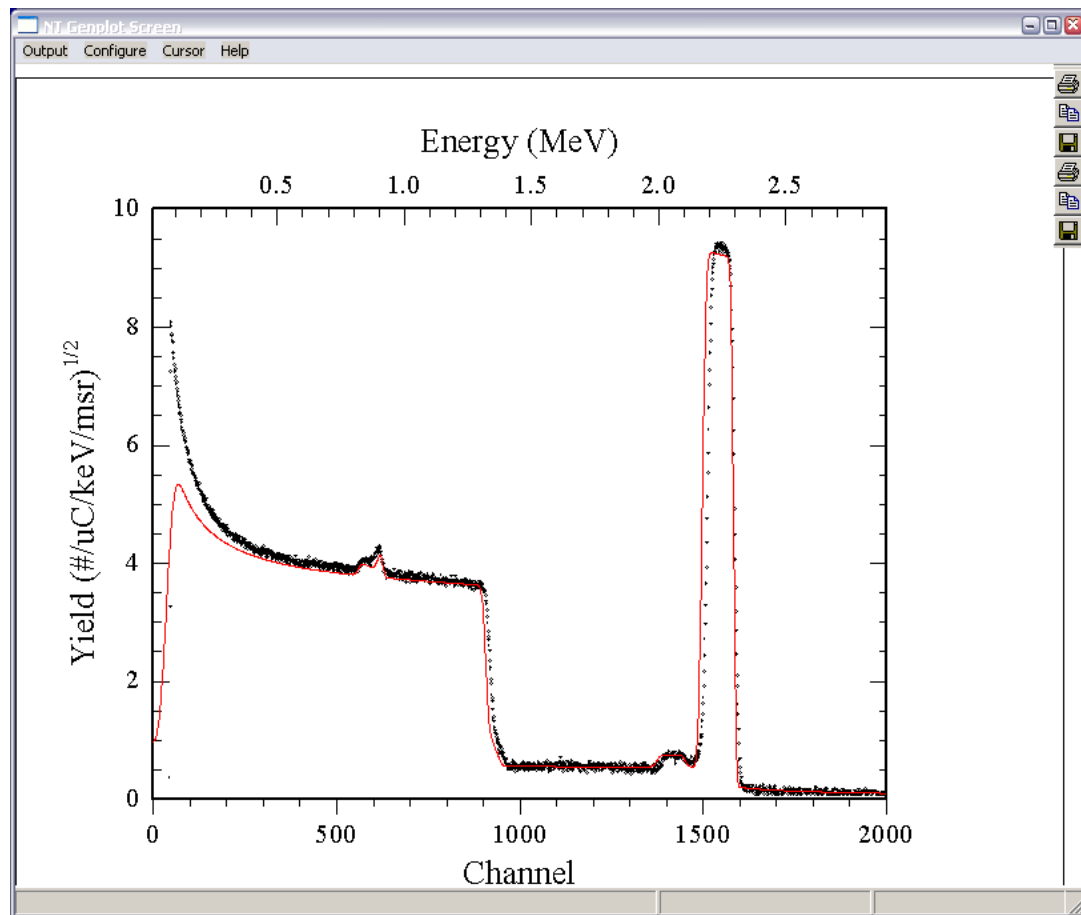
The third step is to define the sample structure. This is made using intuitive easy to learn commands. The corresponding first guess is calculated.



```

XRump
File/Plot Window Layout Edit Variables Help
Your wish? sim
SIM Command: layer 1 comp Hf 1.0 Zr 0.010 O 2 / thick 1000 /cm2
SIM Command: layer 2 comp Si 1 / thick 3 um
SIM Command: show
# Thickness Sublayers Composition
1 1000.00 /CM2 auto Hf 1.000 Zr 0.010
O 2.000
* 2 3.00 um auto Si 1.000
=====
SIM Command: return
Yes Master? plot 1 overlay theory -lt 1
Automatic simulation . fwhm(0.000) . pileup(0.010) . all(0.080) . performed.
Your wish? sim
SIM Command: multiple 1.15 /* Manually match multiple scattering
SIM Command: plot 1 overlay theory -lt 1
Automatic simulation . fwhm(0.000) . pileup(0.010) . all(0.080) . performed.
Here I am! |

```



A manual iterative procedure as described in the first example would follow the first guess. Alternatively, RUMP includes an optimization algorithm. The window shows the definition of the fitting space and the final results. In most situations, not all variables would be fitted at the same time. A combination of manual iterations and fit of some parameters is usual.

```

XRump
File/Plot Window Layout Edit Variables Help
Yes Master? pert
PERT subcommand: normalize 640 890 /* Normalization window in Si
PERT subcommand: window 1350 1700 /* Error window near Zr/Hf
PERT subcommand: window -add 530 640 /* Error window near 0
PERT subcommand: vary comp 1 Zr 0.001 0.02 /* Vary compositions
PERT subcommand: vary comp 1 O 1.5 2.5
PERT subcommand: vary thickness 1 700 1200 /* Vary thicknesses
PERT subcommand: vary tau 1.0 5.0 /* Vary expt parameters
PERT subcommand: vary mev 2.49 2.51
PERT subcommand: vary kev/ch 1.4 1.5
PERT subcommand: vary kev(0) 0 20
PERT subcommand: vary fwhm 10 30
PERT subcommand: fit /* Do the fit

```

CHISQR	comp Zr kev(0)	comp O fwhm	thickness	tau	mev	kev/ch
775.9	0.01	2	1000	2.5	2.5	1.44
	14	16				
414.5	0.01237	2.5	1090	3.22	2.5	1.437
	12.87	30				
78.91	0.01169	2.5	898.8	1.023	2.503	1.436
	20	30				
6.149	0.008874	1.929	846.4	1.694	2.507	1.437
	17.6	22.31				
5.877	0.009212	1.954	845.1	1.891	2.51	1.441
	14.45	19.95				
5.686	0.009279	1.957	846.4	1.976	2.51	1.442
	14.57	20.74				
4.135	0.009247	1.958	845.5	1.962	2.509	1.44
	15.09	21.41				
4.086	0.009226	1.943	839.3	1.89	2.507	1.438
	17.05	22				
3.991	0.009225	1.943	839.2	1.9	2.507	1.438
	17.06	21.61				
3.991	0.009225	1.943	839.2	1.901	2.507	1.438
	17.06	21.57				

```

Variable Value: Sigma
-----
Layer 1, Zr fraction 0.009225005 0.0002770986
Layer 1, O fraction 1.94326 0.007027267
Thickness of layer 1 839.1777 1.390048
MCA time constant (us) 1.901358 0.1051953
Incident energy (MeV) 2.506725 0.0006020225
MCA energy/chan (keV) 1.437939 0.0007441302
MCA chan 0 energy (keV) 17.06374 0.8511739
Detector FWHM (keV) 21.57012 0.2314777

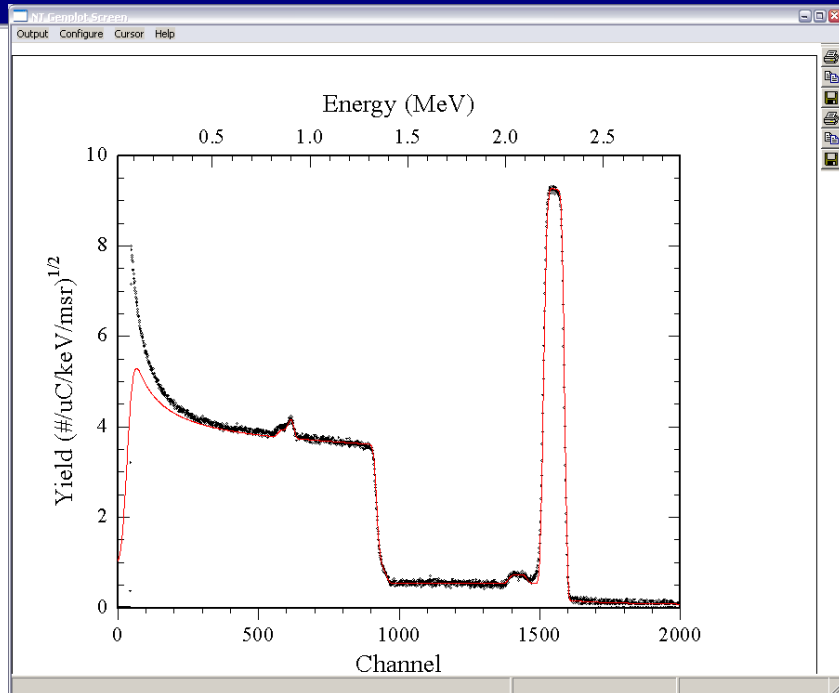
```

Estimated correction factor set for buffer: 0.974769

```

PERT subcommand: plot 1 overlay theory -lt 1
Automatic simulation . fwhm(0.000) . pileup(0.010) . all(0.080) . performed.
Feed me!

```



However, the samples that need to be analyzed are becoming increasingly complex, making stronger demands on data analysis. Advanced physical effects such as roughness, quantum dots and inclusions, multiple and plural scattering, as well as simultaneous use of multiple techniques or different experimental conditions, need to be included in routine data analysis.

RUMP lacks many of these capabilities, which is probably the reason why new generation codes such as SIMNRA are overtaking it.

Other popular first generation codes, used by different groups (as opposed to the many codes that are used mostly by their author only), are GISA (Rauhala, 1984, Saarilahti and Rauhala, 1992) and RBX (Kótai, 1994), which makes a strong emphasis on working with sets of spectra from the same sample.

6. New generation codes - SIMNRA and NDF

Several IBA data analysis codes were developed in the 1990s. Of these, SIMNRA (Mayer, 1997) and NDF (also known as DataFurnace) (Jeynes et al., 2003) put strong emphasis on implementing advanced physics and experimental conditions.

Another code, DEPTH (Szilágyi, 1995), was developed specifically to make state of the art calculations of depth resolution. It is not geared for analysis of data, but it (or a different implementation of the same algorithms) should be used whenever depth resolution is important.

6.1 Further capabilities

The reader is referred to section 3 of this chapter for information about when the effects mentioned here are important.

SIMNRA and NDF both implement plural and multiple scattering effects, to some extent. Multiple scattering is only included insofar as it affects the depth resolution.

SIMNRA includes its own algorithms to calculate the depth resolution. NDF uses a different approach, which is to call in run time DEPTH (NDF writes the required input files automatically), and use the DEPTH results. This has the advantage that DEPTH is state of the art and is still being developed and updated, and the disadvantage that the user must also have DEPTH (which is free of charge) installed.

Both codes have some roughness capabilities. SIMNRA calculates very many different trajectories for actual surfaces, defined by the user. This is accurate, slow, and requires detailed knowledge of the sample surface. NDF uses models for a few types of roughness, and also for inclusions and quantum dots. This is fast, requires less knowledge by the user, but is not as accurate. In practice, the SIMNRA approach is best for detailed studies of a few very important samples, while the NDF approach is adequate for routine analysis of roughness parameters.

SIMNRA includes RBS, ERDA, and non-resonant NRA, for any ion detected at any angle (including forward scattering and transmission), and any target. NDF includes those techniques, as well as PIXE (Pascual-Izarra, 2006a) and resonant NRA.

SIMNRA offers some limited support for multiple spectra collected from the same sample. The user must write a script or small program and use OLE automation, supported by SIMNRA. NDF is designed for analyzing any number of spectra from the same sample. The same depth profile is used to fit simultaneously all the spectra. There are no restrictions on using data from different techniques, and all complementary information is integrated into the final result.

Barradas published recently algorithms to improve the simulation of buried resonances (Barradas et al., 2006), double scattering at grazing angles (Barradas, 2004), the yield at very low energies (Barradas, 2007), and the shape of surface signals in high resolution experiments (Barradas et al., 2007). These effects are at the time of publishing this Handbook only included in NDF, but other codes can easily include them as well.

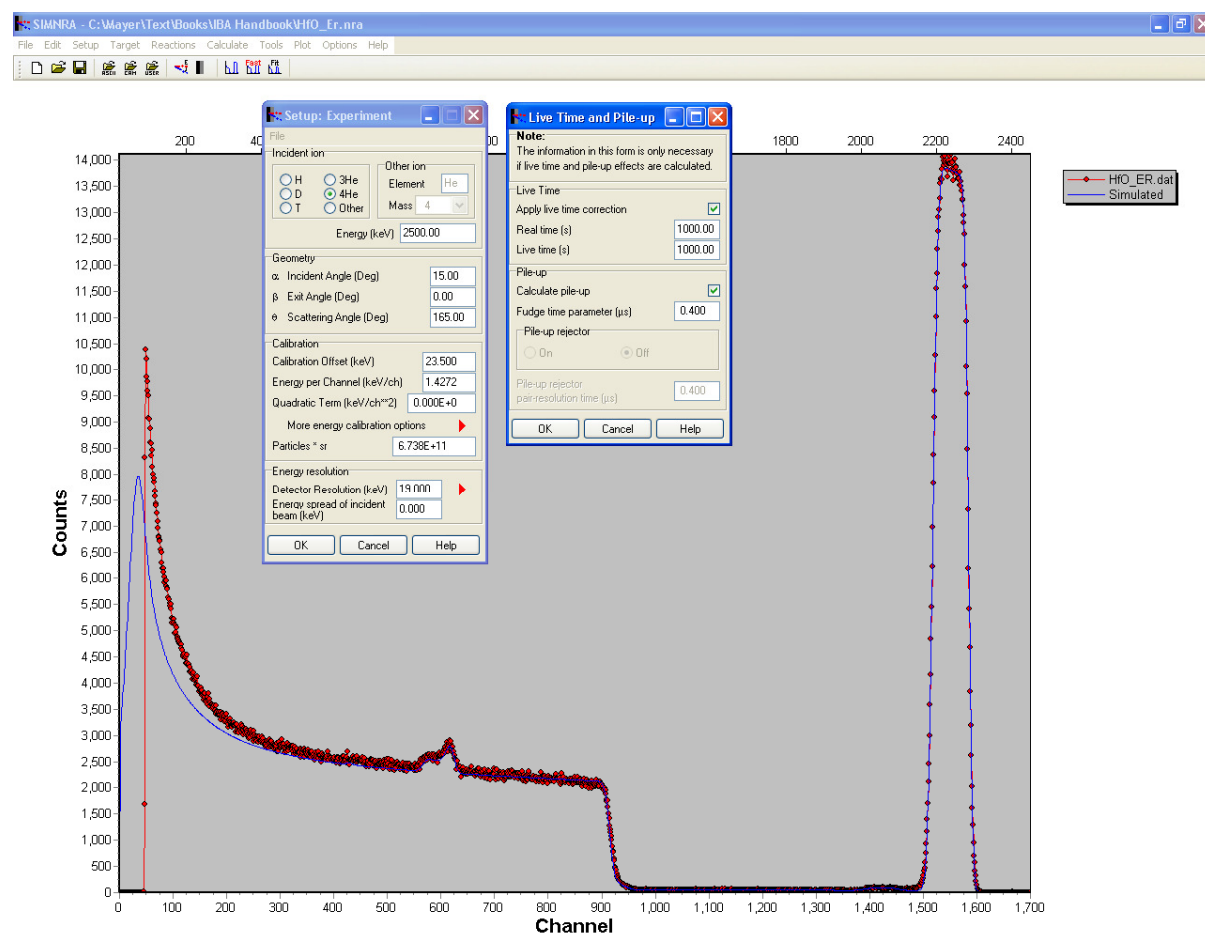
6.2 SIMNRA

Development of SIMNRA started in 1996. It is a Windows code with intuitive menus and windows.

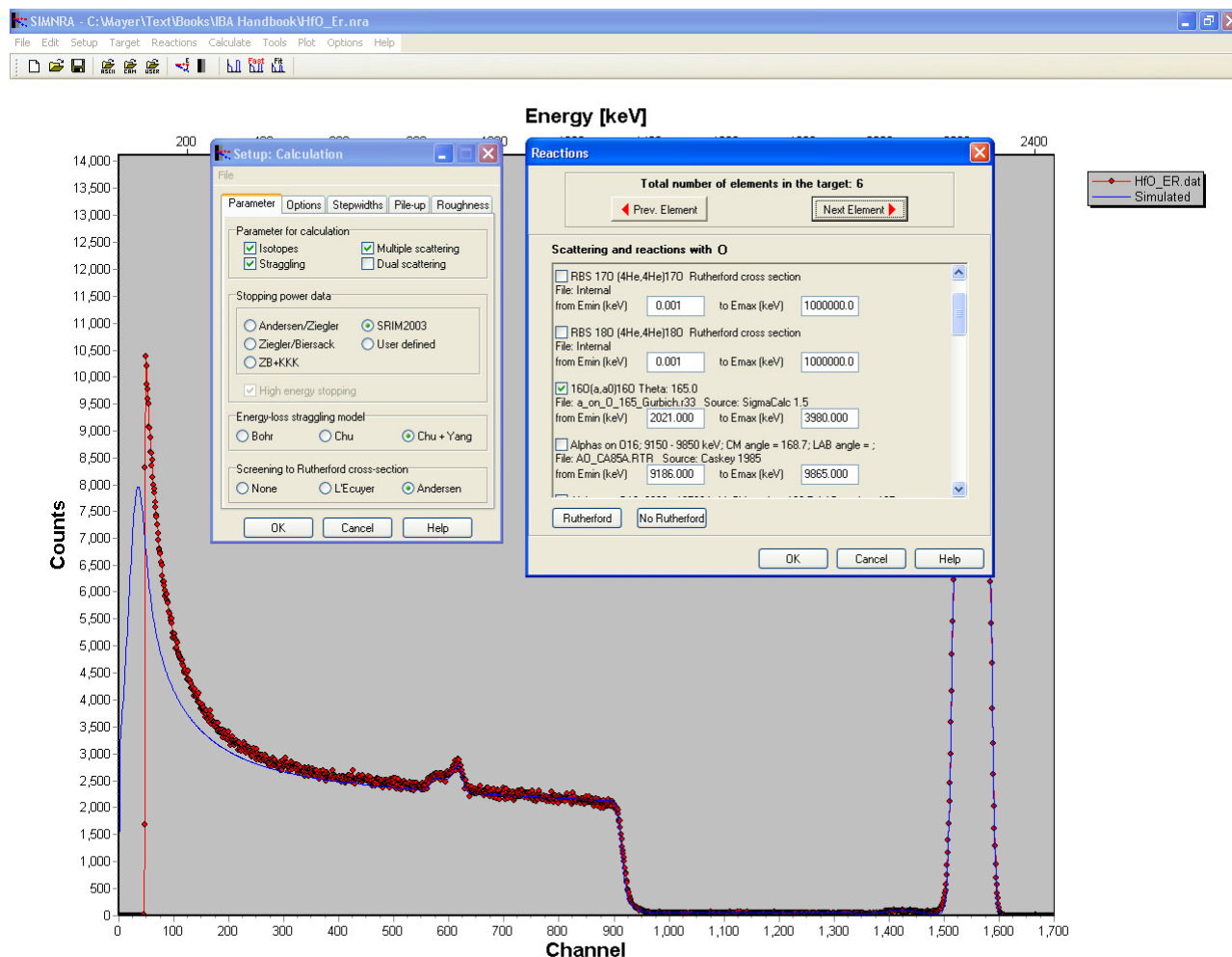
We show in the SIMNRA **worked example DA4** exactly the same spectrum that was used for the RUMP worked example. It is easy to follow how a rather different procedure leads to equivalent results.

Worked example DA4 - SIMNRA

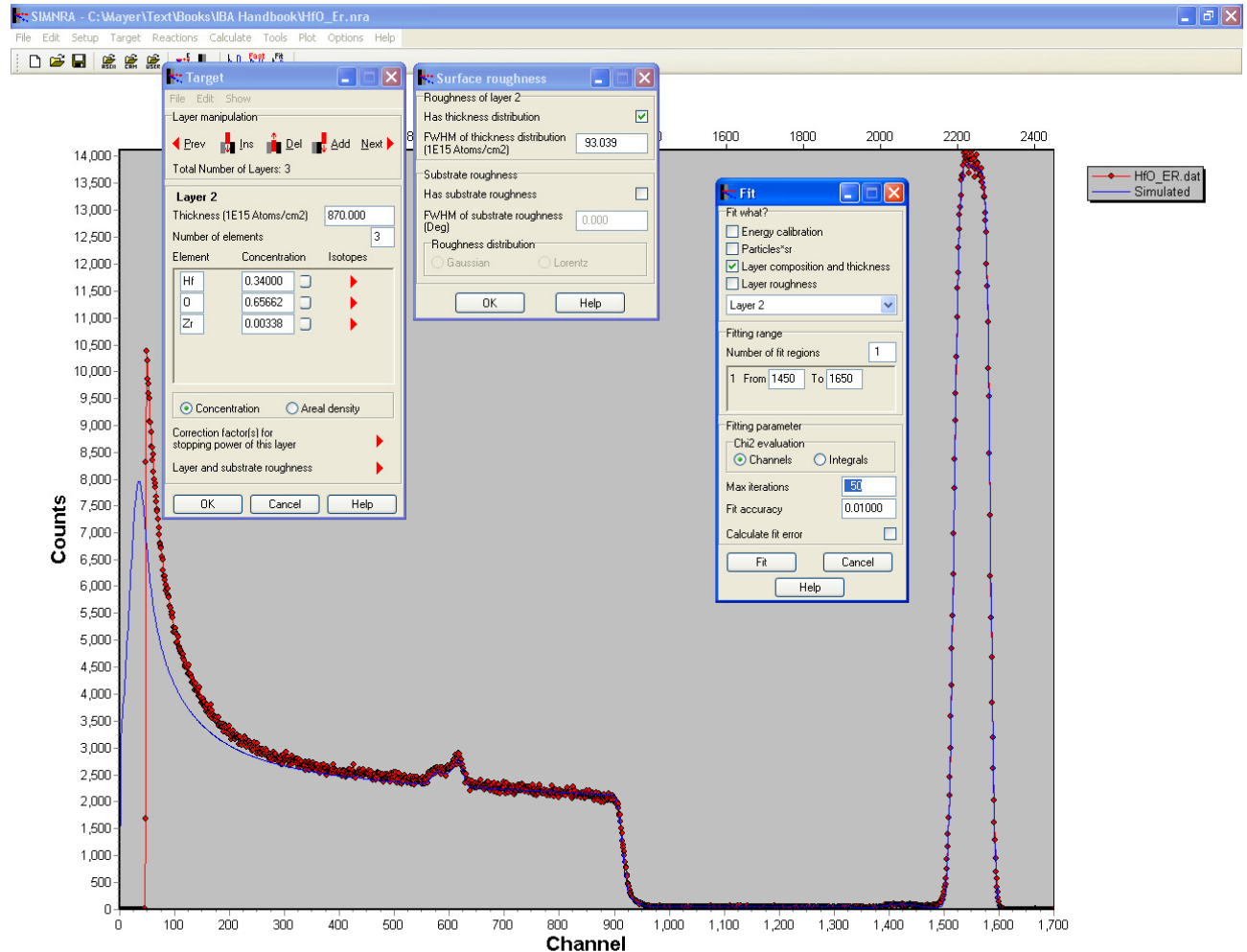
The first step of the analysis, after loading in the data, is to define the experimental conditions. This made in intuitive windows called from the Setup menu. In the example shown, the real and live time are used to apply a live time correction and to calculate the pile-up contribution. The final result of the analysis is already shown here; in a situation where analysis is just starting, only the data would appear.



The second step is to define the physics included in the calculation. In this case, all isotopes are calculated separately (as opposed to making one single calculation for the average mass of the target element), Bohr straggling with the Chu/Yang correction and including multiple scattering is calculated, SRIM2003 stopping powers are used, the scattering cross section for the $^{16}\text{O}(\alpha,\alpha)^{16}\text{O}$ is calculated with SigmaCalc, and Andersen electron screening is calculated for the other elements.



Finally, the sample is defined: layers are created, with any number of elements. The user inputs the thickness and concentration values, and also roughness parameters if required. Then a simulation is generated and compared to the data. The user can then iteratively refine the sample description until a good fit is reached, or use a fitting routine to adjust the thickness and concentration of one layer at the time.



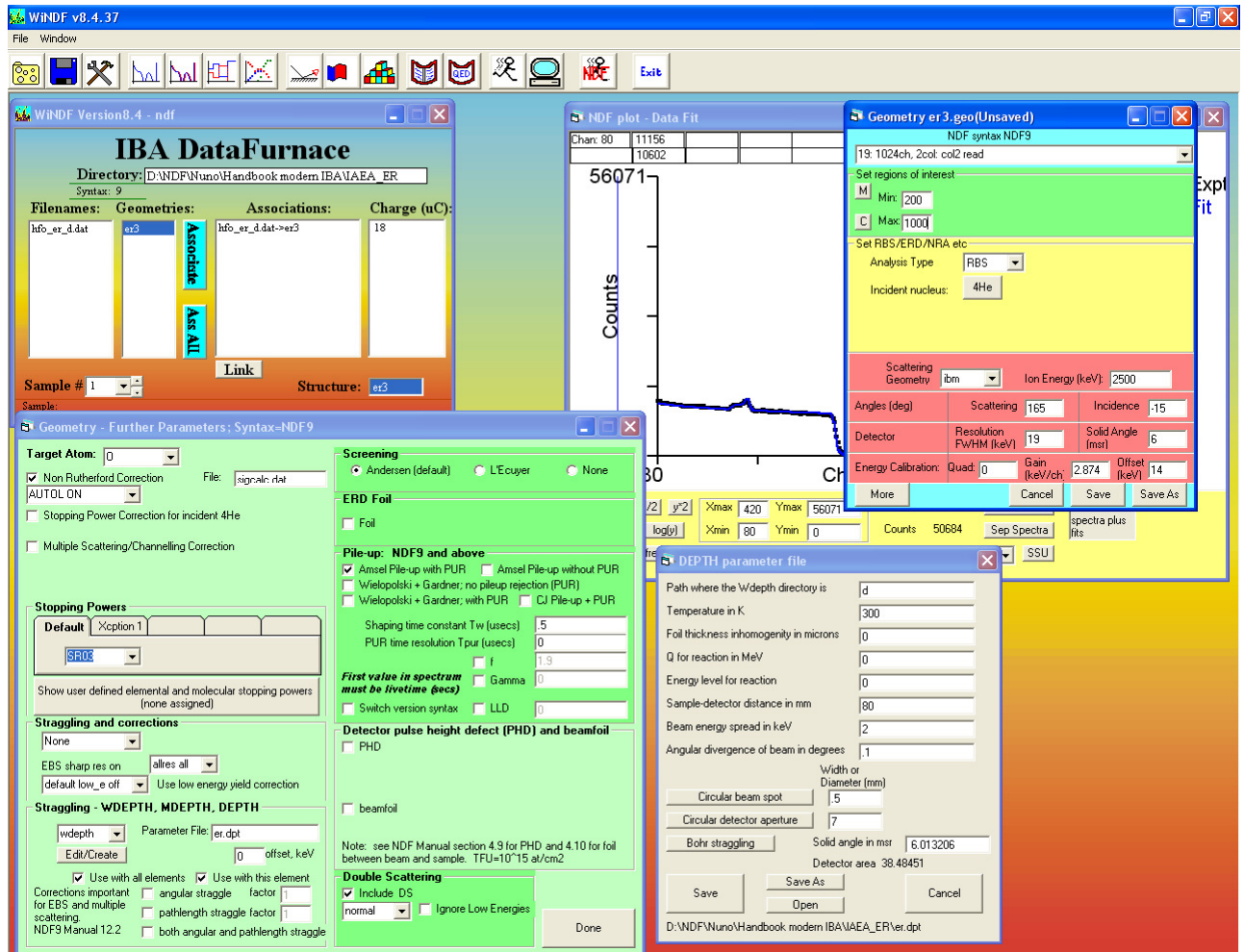
6.3 NDF

Development of NDF started in 1997. It can be run in Windows or DOS mode, in both Windows and UNIX.

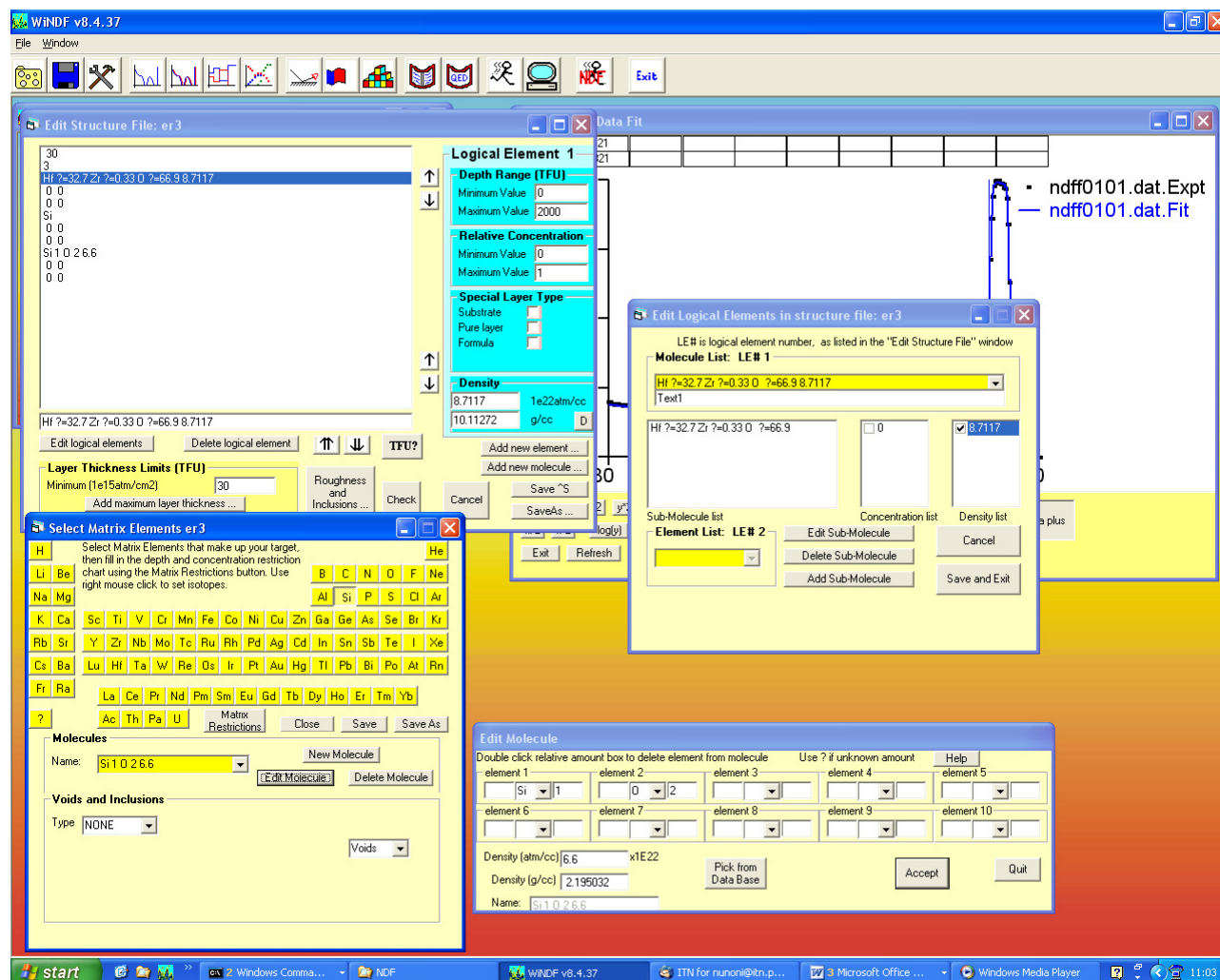
We show in the NDF **worked example DA5** exactly the same spectrum that was used for the RUMP and SIMNRA worked examples. The main difference is that the final depth profile is reached without an initial guess being defined by the user.

Worked example DA5 - NDF/DataFurnace

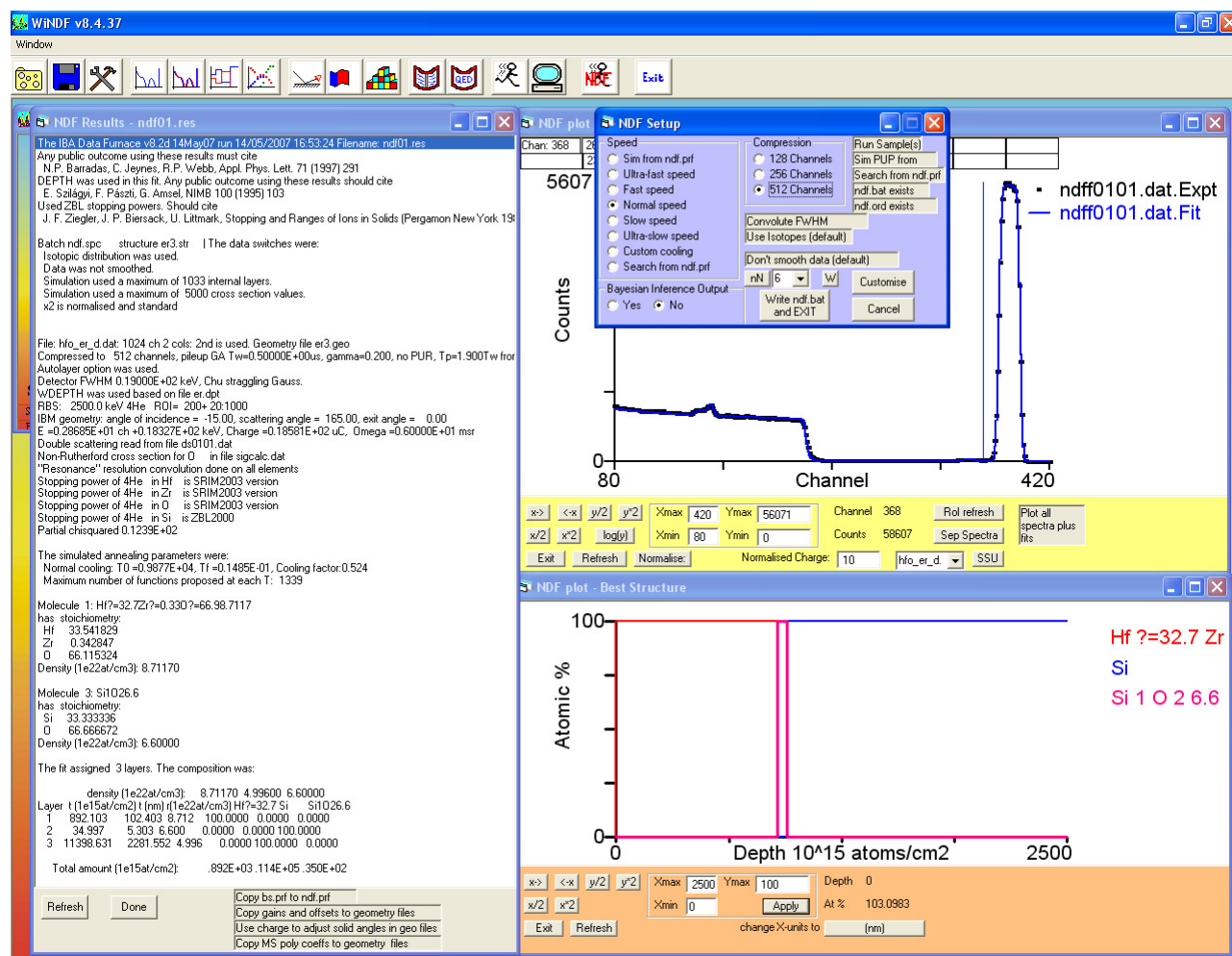
The first step after loading in the data is to define the experimental conditions. This is done by creating geometry files, one per each different set of experimental conditions used. In this case, only one measurement was made so only one geometry is required. The physics included in the calculation (the same as in RUMP and SIMRNA) is also input in the geometry file. Note that NDF does not make its own multiple scattering calculations; instead, it uses DEPTH in run time. The final step is to associate each spectrum to its corresponding geometry, in the main “IBA DataFurnace” window.



The second step is to define which elements exist in the sample. This is made creating a structure file with logical elements, which can be simple elements such as Si, molecules such as SiO₂ with given density, or complex molecules with unknown stoichiometry to be determined in the fit. Restrictions on the depth and concentration ranges where each logical element can exist may be given. If many completely different samples are to be analyzed in batch mode, one structure file is created for each sample. If many similar samples are to be analyzed, the same structure file is used for all of them.



The final step is to run an automated fit. In this case, the user does not have to define a layer structure. This will be an output of the fit. The algorithm used, simulated annealing, tries to find the simplest structure consistent with the data. As it is completely automated, the user must check the results, because it can find unwanted solutions. Alternatively, the user can also make an iterative analysis by defining a layer structure in the usual way. This can also be the initial guess for a local search on all parameters.



6.4 Issues

Both SIMNRA and NDF are actively developed and supported. This means that users can rely on advice and help by the developers.

Both codes are strictly proprietary. The source code is restricted to the authors. This means that users cannot check whether the algorithms used are correct or not. Most users don't want to do that anyway, and the IAEA intercomparison exercise of IBA software showed that the codes are essentially correct.

Both codes are only available commercially. Free test versions can be obtained, but to use the codes in research or industry they must be purchased. This limits their availability. It also means that reliable first generation codes will continue to be used in many cases. This is not a bad thing, since those codes are perfectly capable of handling many experimental data.

Some modules recently introduced in NDF (e.g. for PIXE and resonant NRA) are open source.

New generation codes are more complex and difficult to use, which is normal since they include many further options. This is another reason for the continuing usage of first generation codes in cases where those options are not necessary.

7. Monte Carlo simulation

The standard data analysis procedure described in the sections above, uses deterministic algorithms. These can include more or less physics via accurate or approximative implementations. All of them have limitations coming from two main sources: First, many phenomena are treated in a statistical way with disregard for the real particle-particle interactions that occur. Energy loss, energy loss straggling, and multiple scattering are the three main phenomena in this category. In some cases, such as multiple scattering in grazing angle conditions, the best models available (Amsel et al., 2003) reach their limit of validity. Second, the details of the experimental set-up are normally disregarded. For instance, calculations of geometrical straggling often disregard its influence in the scattering cross section (Szilágyi, 1995, and Rauhala et al., 2006). Details of detection systems other than solid-state dispersive energy detectors, such as TOF systems, are not implemented in most standard codes.

In particular, standard codes have problems in the analysis of heavy ion TOF-ERDA data, particularly at low energies where multiple scattering plays a very important role. Not only are signals broadened, but the actual yield is also not what would be expected from single scattering.

The alternative is to develop a Monte Carlo (MC) simulation of the individual particle-particle interactions. In practice, ion-electron interactions are not calculated, and tabulated stopping powers are used. Nevertheless, complex physical processes such as double and multiple scattering, as well as the full ion-detection system interaction, are taken into account in a natural way, without the approximations that standard codes do.

Two MC codes for general-purpose analysis of ERDA data have been presented recently and applied to the analysis of different systems. MCERD can also handle RBS data (Sajavaara et al., 1998, and Arstila et al., 2001). The second one, FTHIE, is a fast Fortran version of TRIM for heavy ion ERDA (Johnston et al., 2000, and Franich et al., 2004). Other codes, such as for instance RBSIM (Smulders et al., 1987), or using GEANT4 (Geil et al., 2007) also exist.

The **worked example DA6** of data analysis by MC shown illustrates very well the capabilities and limitations of MC. All spectral features are reproduced, which allows the user to ascertain whether a given signal is relevant or not; in the example presented, it is possible to exclude the presence of O in the TaN layer with accuracy much better than what could be achieved by standard codes where plural and multiple scattering are not as accurately calculated as with MC. On the other hand, statistical oscillations are observed in the calculation. They represent the accuracy of the MC calculation, which can be improved by using longer calculation times. Nevertheless, the calculation of backscattered ions, as well as of low energy signals, is inherently slower in MC.

The main barrier to the general use of MC codes in routine data analysis, besides calculation times which are still longer than with standard codes, is that they are considered difficult to use. In some cases, there is no graphical user interface available, and the user must edit input files and look at output files, which is very efficient for advanced users and rather difficult for everyone else. In practice, MC codes are still used almost exclusively by their authors and their close collaborators.

Nevertheless, the extraordinary quality of the simulations that can be achieved, particularly when plural and multiple scattering are important, means that MC may be the basis for the next generation of codes, once user interface and computer speed issues are solved.

Worked example DA6 - Monte Carlo

We show in **Fig. DA9** a TOF measurement of a Si/SiO₂ 100nm/TaN 30nm sample measured with a 16 MeV ⁶³Cu beam, analyzed with MCERD. Recoils and backscattered Cu were separated by the detection system.

The analysis, shown in **Fig. DA10**, leads to Si 1.00±0.02 O 2.00±0.02 and Ta 0.47±0.02 N 0.53±0.02 stoichiometries. The first comment is that the simulations include the statistical fluctuations expected from MC. The most important point is that extraordinarily good agreement with the data is obtained, even in the shape of the signal back edges and the low energy backgrounds. This is essential for instance to rule out the presence of O in the TaN film. No standard code could achieve such results.

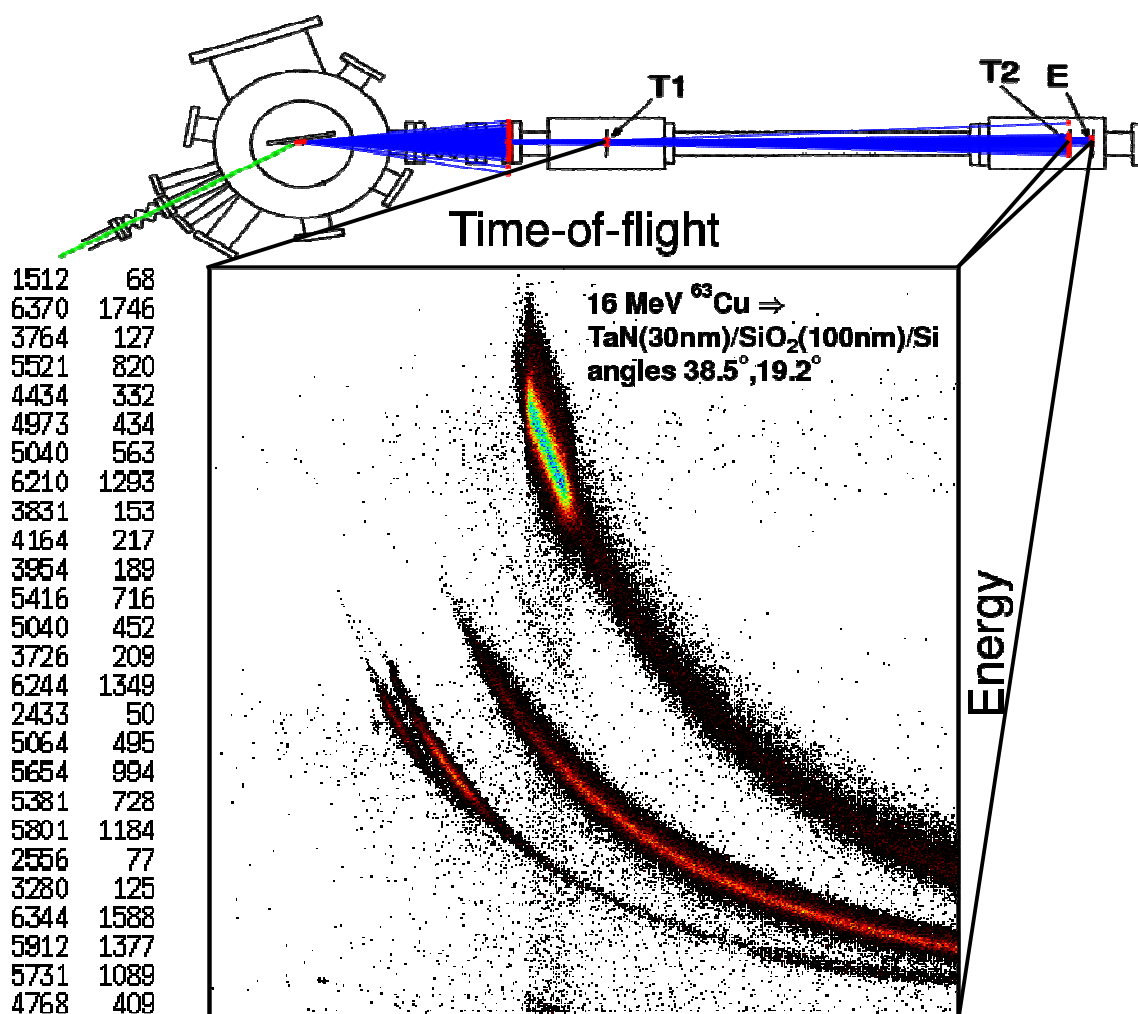


Fig. DA9. Time-of-flight ERDA of a Si/SiO₂ 100nm/TaN 30nm sample measured with a 16 MeV ⁶³Cu beam.

The statistical fluctuation of the simulation is high for the Ta recoil signal. This is due to the low recoil cross section for this heavier target element. Also, the backscattering cross section is low, which means that the calculation of the Cu recoils can be orders of magnitude slower

to reach the same statistical accuracy. This is inherent to MC data analysis. Further improvements in the efficiency of the algorithms and in the computer speed can lead to faster simulation times, which are currently in the minute to hour range.

The Ta recoil signal is not as well simulated as the other elements, and a good simulation requires a slightly smaller layer thickness, which is not consistent with the data from the other elements. This is due to inaccuracies in the heavy ion stopping power data bases, which are sparse and not as accurate as for H and He, particularly at low velocities. This is a problem of the technique and not of the data analysis method, since all codes rely on the same stopping data bases.

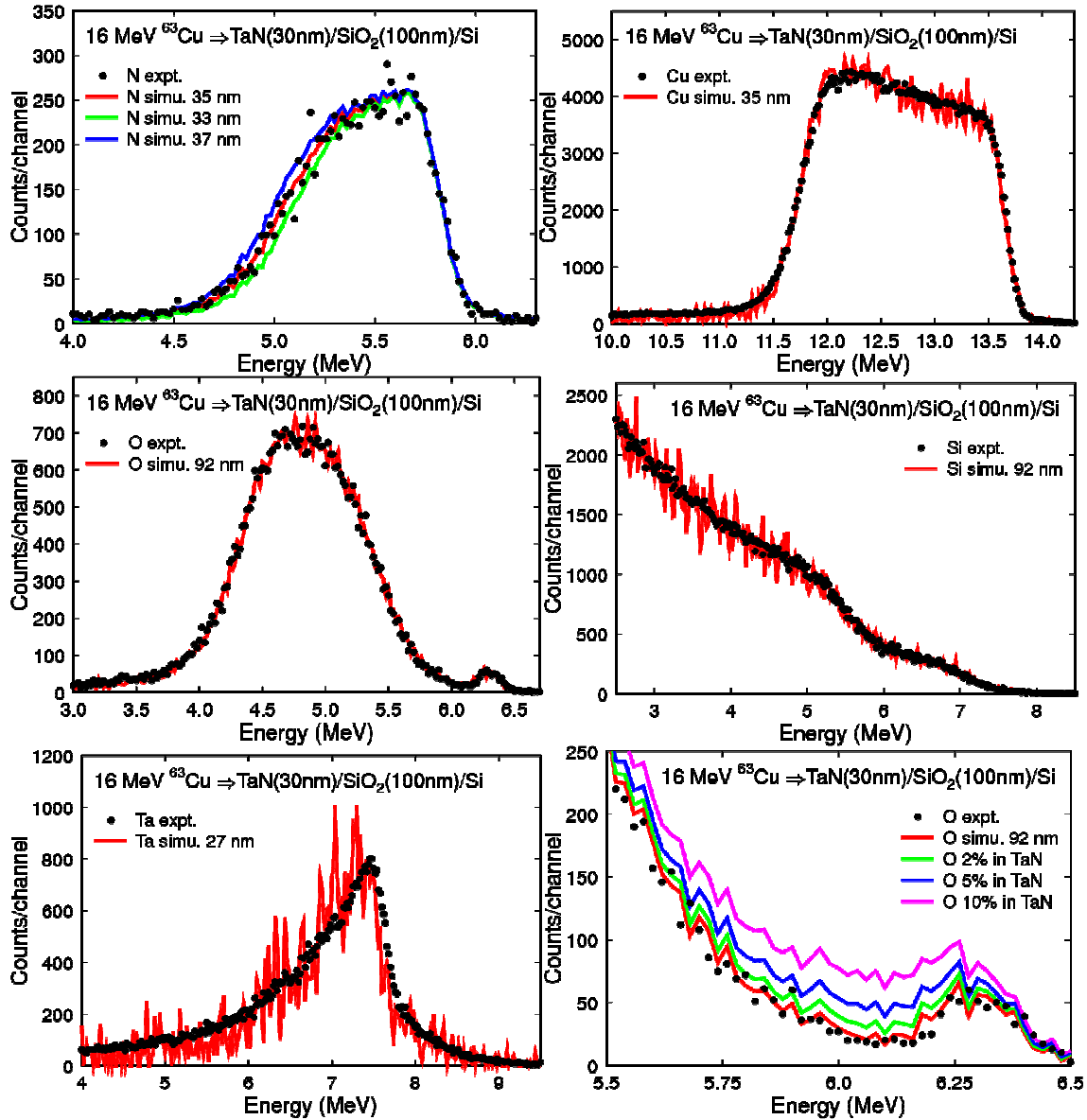


Fig. DA10. MCERD analysis of TOF-ERDA of a Si/SiO₂ 100nm/TaN 30nm sample measured with a 16 MeV ⁶³Cu beam.

8. Other techniques

In this section only a brief mention to methods and codes used for data analysis of other techniques is made.

8.1 PIXE

The PIXE community developed over the years its own methods and codes for data analysis. The IAEA organized an intercomparison exercise of PIXE codes (Blaauw et al., 2002), but only very simple spectra were tested.

The best known is GUPIX (Maxwell et al., 1995), used in many labs around the world. GUPIX is geared towards analyzing PIXE energy spectra accurately, including from multilayered targets. GUPIX is not designed to determine quantitative two dimensional concentration maps from microbeam experiments.

AXIL (Esen et al., 1977) and its free of charge version QXAS are also widely known.

More recently, GeoPIXE was developed (Ryan et al., 1990, and Ryan, 2000). It has proved to be very powerful not only in the analysis of energy spectra, but also for quantitative 2D analysis, and it is also capable of analyzing multilayered targets as well as 3D inclusions by modeling PIXE yields from buried 3D objects.

An alternative approach AXSIA (Doyle et al., 2006) has been recently proposed, using multivariate spectral analysis. This has the advantage of being automated and nonbiased, and can also in principle be used to combine different data sets, such as simultaneously collected micro-PIXE and micro-RBS.

PIXE has been combined with RBS in the same code already in the 1990s, with the so-called “Q factor” method implemented in the DAN32 user-friendly package (Grime, 1996), which uses RUMP and GUPIX. A fit to the proton-RBS spectrum collected simultaneously with the PIXE data is made. This is used to determine the actual collected charge, which is then used in the quantitative analysis of the PIXE data. This very useful improvement, does not however ensure a complete consistency between the analysis of the RBS and PIXE data, and it also does not fully take advantage of the combination of the depth sensitivity of RBS with the elemental and trace sensitivity of PIXE.

The open source LibCPIXE library (Pascual-Izarra et al., 2006b), based on the DATTPIXE code (Reis et al., 1992), also supports multilayered targets. It has been integrated in the general purpose IBA data analysis code NDF (Jeynes et al., 2003). Any number of PIXE spectra can be analyzed together with any number of RBS, ERDA and NRA spectra, leading to one single depth profile consistent with all data. It is, as GUPIX, geared towards spectra and not 2D maps.

8.2 Resonant NRA, PIGE, NRP, MEIS, channeling, microscopies, etc.

This short section is dedicated to techniques and experimental conditions not covered above. In several different techniques the yield of a given nuclear reaction is determined as a function of initial beam energy. Depth profile information can be extracted from the shape of the excitation curve obtained by scanning the beam energy.

The nuclear reaction is often a (elastic or inelastic) particle-particle reaction, or a particle-gamma reaction. These are often called resonant NRA and PIGE, respectively. Different

codes have been presented, such as ANALNRA by Johnston (1993), WinRNRA by Landry et al. (2001) and ERYA by Mateus et al. (2005).

If a narrow resonance is used, normally isolated and background-free, together with a correspondingly small initial beam energy spread (both with FWHM typically smaller than 0.5 keV) the term Narrow Resonance Profiling (NRP) is used independently of the reaction type. In that case, it is necessary to take into detailed account the individual energy loss events to correctly calculate the excitation curves. The best-known code for that purpose is SPACES by Vickridge et al. (1990). It implements the stochastic theory of energy loss of Maurel et al. (1982), which allows the user to retrieve accurately high resolution depth profiles. Codes that assume a Gaussian energy distribution of the beam will lead to inaccurate depth profiles, particularly near the surface. Recently, another code, FLATUS, has been presented by Pezzi et al. (2005).

Medium Energy Ion scattering (MEIS) could be seen as a particular case of RBS at low energies, but in fact several important points must be considered, including special detector arrangements, the screened scattering cross section used, and also that for the high resolution profiling that can be made with MEIS, stochastic energy loss must be considered (Pezzi et al., 2007).

Specific methods have been developed for the analysis of channeling data. This includes dedicated Monte Carlo codes (sometimes limited to specific systems) as well as different implementations of analytical theories. Monte Carlo codes such as FLUX by Smulders et al. (1987), or BISIC (Albertazzi et al., 1996) are adequate for detailed studies of the crystalline lattice, including lattice location of impurities, defect configuration and damage. Analytic codes such as DICADA (Gärtner, 2005) or RBX (Kótai, 1994) are less accurate but possibly easier to use in the study of defect profiles. RBX is the only standard all-purpose data analysis code that includes channeling.

Different ion-based microscopies have been developed. These range from the 2D maps collected with PIXE to techniques such as STIM. They all have dedicated methods of data analysis. Particular applications often require the development of specific methods. These are outside the scope of this chapter.

Artificial neural networks have been developed by Barradas, Vieira, and co-workers for the unattended automatic analysis of IBA data, and applied to a variety of systems, from the very simple to the very complex (Barradas et al., 2000, Nené et al., 2006). This can only be of practical importance when large numbers of similar spectra are collected, as for instance in quality control applications, or for analysis of data collected in real-time RBS experiments, where hundreds or thousands of spectra are collected within a few days.

Finally, many codes and data analysis codes have been developed over the years for very specific applications and experimental conditions. We refer the reader to the review paper Rauhala et al. 2006 and references thereof, where several of these codes are discussed.

Acknowledgements

We would like to thank Mike Thompson, Matej Mayer, and Kai Arstila for providing the figures for the RUMP, SIMNRA and MCERD worked examples, as well as all those who commented on early drafts.

TABLE 1. General information about analysis programs.

Analysis Program	Technical Contact	Current Status	Distribution Mode	Status of source code	Operating Systems
DEPTH	Edit Szilágyi KFKI Research Institute for Particle and Nuclear Physics Budapest, Hungary szilagyi@rmki.kfki.hu ; www.kfki.hu/~ionhp/	Active Development	No charge. Downloadable from the WEB.	Restricted to author -not available.	DOS and Windows
GISA	Eero Rauhala University of Helsinki, Helsinki, Finland and Jaakko Saarilahti, Technical Research Center of Finland Eero.rauhala@helsinki.fi ; Jaakko.Saarilahti@vtt.fi	In Use	No charge. Write to author for copy.	Restricted to author -not available.	DOS (or emulators)
MCERD	Kai Arstila IMEC, Leuven, Belgium kai.arstila@iki.fi	Active Development	No charge. Write to author for copy.	Source code available.	Linux (Windows)
NDF (DataFurnace)	Nuno Barradas Technological and Nuclear Institute Sacavém, Portugal nunoni@itn.pt ; www.ee.surrey.ac.uk/Research/SCRIBA/ndf/	Active Development	Commercial through Univ. of Surrey Evaluation copies available by request.	Restricted to author -not available. Some modules open source.	Windows, DOS, UNIX
RBX	Endre Kótai KFKI Research Institute for Particle and Nuclear Physics Budapest, Hungary kotai@rmki.kfki.hu	Active Development	No charge. Write to author for copy.	Restricted to author -not available.	Windows
RUMP	Mike Thompson Dept. of Materials Science, Cornell University Ithaca, NY USA motl@cornell.edu ; www.genplot.com	Active Development	Commercial through Computer Graphics Service Evaluation copies available on WEB.	Source code available.	Windows, Linux, UNIX, OS2
SIMNRA	Matej Mayer MPI for Plasma Physics Garching, Germany Matej.Mayer@ipp.mpg.de ; www.rzg.mpg.de/~mam/	Active Development	Commercial through MPI for Plasma Physics Evaluation copies available on WEB.	Restricted to author -not available.	Windows

TABLE 2. User interface properties of the analysis programs.

Analysis Program	Primary Interface "nature"	Primary simulation modes	Graphic Output
DEPTH	Interactive or batch	Manual iteration	N/A
GISA	Interactive	Manual iteration; automated parameter search	Screen only
MCERD NDF (DataFurnace)	Batch Batch directed or interactive	Manual iteration Fully automated search; manual iteration	N/A Publication quality
RBX	Interactive	Manual iteration	Draft quality
RUMP	Interactive	Manual iteration; automated parameter search	Publication quality
SIMNRA	Interactive	Manual iteration; automated parameter search	Draft quality

TABLE 3. Fundamental databases used by analysis programs.

Analysis Program	Stopping powers	Cross Sections
DEPTH	ZBL'95	User defined from file.
GISA	TRIM1991 or Ziegler and Chu ; User defined correction per layer.	User defined from file.
MCERD NDF (DataFurnace)	ZBL'96 or user defined ZBL'95, SRIM, KKKNS (Si), MSTAR. Ability to load other values; user defined correction per ion/element.	Rutherford, user defined from file to be included. User defined from file.
RBX	ZBL'95 With channeling correction possible; User defined correction per layer.	Internal (modifiable) library of cross sections; external Cross-section Library Editor (import Sigabase R33; user defined).
RUMP	ZBL'92, SRIM, KKKNS User defined compounds and databases, user defined correction per layer or per element.	IBANDL, SigmaCalc; user defined.
SIMNRA	Either, SRIM1997, SRIM, or KKKNS, user defined correction per layer and ion.	IBANDL, SigmaCalc; user defined.

TABLE 4. Fundamental physics handled in the simulations

Analysis Program	Isotope Calculation	Screening Calculation	Straggling models	Plural Scattering	Multiple Scattering	Geometric Straggling	Channeling
DEPTH	Single isotope	Yes	Bohr, Chu, Yang, Tschalär	None	Yes. Pearson VII distribution	Yes	No
GISA	Natural abundance and/or specific isotopes	Energy/Angle - external tables by users	Bohr + Lindhard/Scharff	None	None	No	No
MCERD	Natural abundance and/or specific isotopes	No	Bohr, Chu, Yang	Full MC calculation	Full MC calculation	Yes	No
NDF (DataFurnace)	Natural abundance and/or specific isotopes	Energy/Angle – Andersen and L’Ecuyer	Bohr, Chu, Yang, Tschalär	Dual scattering approx. (run time option)	Yes - Gaussian approximation from DEPTH calculation	Yes - from DEPTH calculation	No
RBX	Natural abundance and/or specific isotopes	Yes	Bohr, Chu, Yang, Tschalär	None	Yes (same model as DEPTH)	Yes	Defect Calculation Simulation of Channeled spectra
RUMP	Natural abundance and/or specific isotopes	Energy only - L’Ecuyer	Bohr	None	None	No	No
SIMNRA	Natural abundance and/or specific isotopes	Energy/Angle - Andersen and L’Ecuyer	Bohr, Chu, Yang, Tschalär	Dual scattering approx. (run time option)	Yes (DEPTH model approximated as Gaussian)	Yes	No

TABLE 5. Experimental conditions and simulation capabilities.

Analysis Program	Incident Ions	Analytical Techniques	Scattering Geometries	Pileup correction	Detection Systems	Stopper Foils	Energy calibration
DEPTH	All	RBS, ERDA, NRA	IBM, Cornell	No	Energy dispersive (magnetic spectrograph coming)	Simulated; including inhomogeneities	Linear
GISA	All	RBS	IBM	No	Energy dispersive	N/A	Quadratic
MCERD	All	ERDA, RBS	IBM	No	Energy dispersive, TOF, different layers in detector for e.g. gas detectors	Simulated; equivalent treatment to sample	Linear
NDF (DataFurnace)	All	RBS, ERDA, non-resonant NRA, PIXE, NDP, resonant NRA	IBM, Cornell, General	Yes	Energy dispersive	Simulated; equivalent treatment to sample	Quadratic; varying by ion species
RBX	All	RBS, ERDA, non-resonant NRA	IBM, Cornell	Yes	Energy dispersive	Simulated; Homogeneous foils only	Linear
RUMP	All	RBS, ERDA	Cornell, IBM, General	Yes	Energy dispersive, partial TOF	Simulated, or from user calibration	Linear
SIMNRA	All	RBS, ERDA, non-resonant NRA	IBM, Cornell, General	Yes	Energy dispersive, TOF, electrostatic, thin solid state detectors with transmission of particles	Simulated; equivalent treatment to sample	Quadratic; varying by ion species

TABLE 6. Fitting capabilities (DEPTH and RBX have no fitting capabilities).

Analysis Program	Starting conditions	Optimization method	Error estimation	Statistics used	Searchable experimental parameters	Auto-refinement of layers	Limitations
GISA	Reasonable guess	χ^2 minimization	None returned		None	No	One layer at a time
NDF (DataFurnace)	Elements only; guess can be used but not required	Simulated annealing plus grid search	Bayesian inference with Markov chain Monte Carlo integration (time intensive)	Poisson	E_0 , E_{cal} , charge, θ , Φ , φ	Yes	All parameters variable, user controls which ones change
RUMP	Reasonable guess	Marquart search	Curvature of chi-square matrix; full correlation of error sensitivities (intrinsic in search method)	Poisson	E_0 , E_{cal} , charge, current, θ , Φ , φ	No	No internal limit, practical of 30 parameters at a time
SIMNRA	Reasonable guess	Simplex search	Additional search to determine curvature near best fit (comparable to fit time)	Poisson	E_{cal} , charge	No	One layer at a time, all characteristics

TABLE 7. Sample definition and complexity handled.

Analysis Program	Sample Description	Continuous Profiles	Slab Limitations /Elements	Substrate Roughness	Layer Roughness
DEPTH	Layer definition	Slabs only	None	No	No
GISA	Layer definition or profile function	Maps continuous profiles onto slab structure	10 layers; 10 elements; User can define so layer*elem. is constant	No	No
MCERD					
NDF (DataFurnace)	Layer definition; limited use of profile function	Effective error function interdiffusion profiles between layers.	250 layers in description; up to 92 constituents	Yes - approximated as energy broadening	Yes - approximated as energy broadening
RBX	Layer definition	User defined functions (Gauss, error functions etc.). Channeling defect distributions.	None	No	No
RUMP	Layer definition with equation overlays	Gaussian implants, error function diffusion, Pearson IV profiles, one-sided and two-sided diffusion.	None	No	Yes - single or dual sided, all interfaces possible.
SIMNRA	Layer definition	Slabs only	100 layers in description; 40 elements per layer	Yes - Lorentzian or Gaussian angular distribution	Yes, all interfaces possible.

Table 8. The effect of some phenomena on data analysis.

<i>phenomenon</i>	<i>ion</i>	<i>energy</i>	<i>scattering angle</i>	<i>target element</i>	<i>effect on spectrum</i>	<i>error</i>	<i>effect on analysis</i>
cross section							false quantitative analysis
electron screening	all	all	<15°	all	decreased yield	unknown (large)	
	all	> 150 keV/Z ₁	>15°	heavy		1%	
	all	> 500 keV/Z ₁	>90°	heavy		≥0.2%	
nuclear effects	p	≥ 100 keV	all	light (medium heavy)	increased or decreased yield	depends on reaction (can be large)	
	α	≥ 2.0 MeV	all	light			
stopping power							false quantitative and depth analysis
general uncertainties ¹⁾	p			all	increased or decreased yields and widths	4.2% average (>10% for 13% of target atoms)	
	α			all		4.1% average (>10% for 11% of target atoms)	
	α			Si		≤2%	
	Li			all		5.1% average (>10% for 17% of target atoms)	
	heavier ions			all		6.1% average (>10% for 18% of target atoms)	
Bragg rule violations	all			light compounds (insulators)	increased or decreased yields and widths	≤10-15%	
physical state effects	all			light solids vs. liquid or gaseous	increased or decreased yields and widths	≤5-10%	
energy spread, multiple scattering	heavy		grazing angle geometry		increased or decreased edge and peak broadness	large	false interdiffusion, mixing, depth profile, and roughness analysis
	p		normal incidence			small	
	all		all			depends on details (can be small or large)	
surface roughness	all			all	increased edge and peak broadness	depends on details (can be small or large)	false analysis of intermixing and interdiffusion
channeling	all		incidentally aligned geometry		decreased yields	depends on details (can be small or large)	false quantitative and depth analysis
pulse pile-up	all			heavy (all)	increased or decreased yields, background	≤2-5% for count rates below ≈5 kHz	false quantitative analysis, reduced sensitivity
low energy background	all	low (all)	grazing geometry (all)	heavy (all)	increased background	depends on the details; can be dominant at low energies; small in most analyses	false quantitative analysis, reduced sensitivity

1) The errors quoted refer to SRIM 2003.

Software websites

This list of web sites relevant for IBA software and data analysis is by no means complete. Several of the codes mentioned in this chapter have no dedicated web site.

DEPTH <http://www.kfki.hu/~ionhp/doc/prog/wdepth.htm>

FLUX <http://members.home.nl/p.j.m.smulders/FLUX/HTML/>

GeoPIXE <http://www.nmp.csiro.au/GeoPIXE.html>

GUPIX <http://pixe.physics.uoguelph.ca/gupix/main/>

IBANDL <http://www-nds.iaea.org/ibandl/>

Ion Beam Information System (includes links to several codes) <http://www.kfki.hu/~ionhp/>

LibCPIXE <http://sourceforge.net/projects/cpixe>

MSTAR <http://www.exphys.uni-linz.ac.at/stopping/>

NDF http://www.itn.pt/facilities/lfi/ndf/uk_lfi_ndf.htm

DataFurnace <http://www.ee.surrey.ac.uk/SCRIBA/ndf/>

QXAS <http://www.iaea.org/OurWork/ST/NA/NAAL/pci/ins/xrf/pciXRFdown.php>

RUMP <http://www.genplot.com>

SigmaCalc <http://www-nds.iaea.org/sigmacalc/>

SIMNRA <http://www.rzg.mpg.de/~mam/>

SRIM <http://www.srim.org>

References

Albertazzi, E., Bianconi, M., Lulli, G., Nipoti, R., Cantiano, M. (1996), *Nucl. Instrum. Methods* **B118**, 128.

Alkemade, P.F.A., Habraken, F.H.P.M., van der Weg, W.F. (1990), *Nucl. Instrum. Methods* **B45**, 139.

Amsel, G. (1996), *Nucl. Instrum. Methods* **B118**, 52.

Amsel, G., Battistig, G., L'Hoir, A. (2003), *Nucl. Instrum. Methods* **B201**, 325.

Andersen, H.H., Besenbacher, F., Loftager, P. and Möller, W. (1980), *Phys. Rev.* **A21**, 1891.

Arstila, K., Sajavaara, T., Keinonen, J. (2001), *Nucl. Instrum. Methods* **B174**, 163.

- Barradas, N.P., Jeynes, C., Jenkin, M., Marriott, P.K. (1999), *Thin Solid Films* **343-344**, 31.
- Barradas, N.P. and Vieira A. (2000), *Phys. Rev.* **E62**, 5818
- Barradas, N.P. (2004), *Nucl. Instr. Methods* **B225**, 318.
- Barradas, N.P., Alves, E., Jeynes, C., Tosaki, M. (2006), *Nucl. Instrum. Methods* **B247**, 381.
- Barradas, N. P. (2007), *Nucl. Instrum. Methods* **B261**, 418.
- Barradas, N. P., Pezzi, R.P., Baumvol, I. J. R. (2007), *Nucl. Instrum. Methods* **B261**, 422.
- Barradas, N.P., Arstila, K., Battistig, G., Bianconi, M., Dytlewski, N., Jeynes, C., Kótai, E., Lulli, G., Mayer, M., Rauhala, E., Szilágyi, E., Thompson, M. (2007c), *Nucl. Instr. Methods* **B262**, 281.
- Bichsel, H (2006), *Nucl. Instrum. Methods* **A562**, 154.
- Blaauw, M., Campbell, J.L., Fazinić, S., Jakšić, M., Orlic, I., Van Espen, P. (2002), *Nucl. Instrum. Methods* **B189**, 113.
- Bohr, N. (1948), *Math. Phys. Medd. Vid. Selsk.* **18 (8)**.
- Børghesen, P., Behrisch, R. and Scherzer, B.M.U. (1982), *Appl. Phys.* **A27**, 183.
- Boudreault, G., Jeynes, C., Wendler, E., Nejim, A., Webb, R.P., and Wätjen, U. (2002), *Surf. Interface Anal.* **33**, 478.
- Butler, J.W. (1990), *Nucl. Instrum. Methods* **B45**, 160.
- Chu, W.K. (1976), *Phys. Rev.* **A13**, 2057.
- NDF (2007), The University of Surrey Ion Beam Centre IBA NDF Users Guide, University of Surrey Ion Beam Centre, <http://www.ee.surrey.ac.uk/SCRIBA/ndf/>
- Doolittle, L.R. (1985), *Nucl. Instrum. Methods* **B9**, 344.
- Doyle, B.L., Provencio, P.P., Kotula, P.G., Antolak, A.J., Ryan, C.G., Campbell, J.L., Barrett (2006), *Nucl. Instrum. Methods* **B249**, 828.
- Eckstein, W., Mayer, M. (1999), *Nucl. Instrum. Methods* **B153**, 337.
- Edelmann, E., Arstila, K., Keinonen, J. (2005), *Nucl. Instrum. Methods* **B228**, 364.
- Espen, P. Van, Nullens, H., and Adams, F. (1977), *Nucl. Instrum. Methods* **145**, 579.
- Franich, R.D., Johnston, P.N., Bubb, I.F. (2004), *Nucl. Instrum. Methods* **B19-2208**, 87.
- Gardner, R.P., Wielopolski, L. (1977), *Nucl. Instrum. Methods* **140**, 289.

- Gärtner, K. (2005), *Nucl. Instrum. Methods* **B227**, 522.
- Geil, R.D., Mendenhall, M., Weller, R.A., and Rogers, B.R. (2007), *Nucl. Instrum. Methods* **B256**, 631.
- Genplot, <http://www.genplot.com/>
- Grime, G.W. (1996) , *Nucl. Instrum. Methods* **B109/110**, 170.
- Gurbich, A.F. (1997), *Nucl. Instrum. Methods* **B129**, 311.
- Gurbich, A.F. (1998), *Nucl. Instrum. Methods* **B145**, 578.
- Gurbich, A.F. (2005), in “Nuclear Data for Science and Technology, AIP Conf. Proc. vol. 769” (R.C. Haight, M.B. Chadwick, T. Kawano, P. Talou, eds.), p. 1670. Melville, New York.
- Harjuoja, J., Väyrynen, S., Putkonen, M., Niinistö, L., Rauhala, E., *Appl. Surf. Sci.* 253 (2007) 5228.
- Jeynes, C., Barradas, N. P., Rafla-Yuan, H., Hichwa, B. P., Close, R. (2000a), *Surf. Interface Analysis* **30**, 237.
- Jeynes, C., Barradas, N. P., Wilde, J. R., and Greer, A. L. (2000b), *Nucl. Instrum. Methods* **B161-163**, 287.
- Jeynes, C., Barradas, N.P., Marriott, P.K., Boudreault, G., Jenkin, M., Wendler, E. and Webb, R.P. (2003), *J. Phys. D: Appl. Phys.* **36**, R97.
- Jeynes, C., Peng, N., Barradas, N.P., and Gwilliam, R.M. (2006), *Nucl. Instrum. Methods* **B249**, 482.
- Johnston, P.N. (1993), *Nucl. Instrum. Methods* **B79**, 506.
- Johnston, P. N., Franich, R. D., Bubb, I. F., El Bouanani, M., Cohen, D. D., Dytlewski, N., and Siegele, R. (2000), *Nucl. Instrum. Methods* **B161-163**, 314.
- Kirkpatrick, S., Gelatt, C.D. and Vecchi, M.P. (1983), *Science* **220**, 671.
- Kótai, E. (1994), *Nucl. Instrum. Methods* **B85**, 588.
- Landry, F., and Schaaf, P. (2001), *Nucl. Instrum. Methods* **B179**, 262.
- L'Ecuyer, J., Davies, J.A., Matsunami, N. (1979), *Nucl. Instrum. Methods* **160**, 337.
- Mateus, R., Jesus, A.P., and Ribeiro, J.P. (2005), *Nucl. Instrum. Methods* **B229**, 302.
- Maurel, B., Amsel, G., and Nadai, J.P. (1982), *Nucl. Instrum. Methods* **197**, 1.
- Maxwell, J.A., Teesdale, W.J., and Campbell, J.L. (1995) , *Nucl. Instrum. Methods* **B95**, 407.

Mayer, M. (1997), Technical Report IPP9/113, Max-Planck-Institut für Plasmaphysik, Garching, Germany.

Mayer, M. (2002), *Nucl. Instrum. Methods* **B194**, 177.

Mayer, M., Fischer, R., Lindig, S., von Toussaint, U., Stark, R.W., and Dose, V. (2005), *Nucl. Instrum. Methods* **B228**, 349.

Mayer, M. (2007), SIMNRA User's Guide, Max-Planck-Institut für Plasmaphysik, <http://www.rzg.mpg.de/%7Emam/>

Nené, N. R., Vieira, A., Barradas, N.P. (2006), *Nucl. Instrum. Methods* **B246**, 471

Neumaier, P., Dollinger, G., Bergmaier, A., Genchev, I., Görgens, L., Fischer, R., Ronning, C., Hofsäss, H. (2001), *Nucl. Instrum. Methods* **B183**, 48.

Padayachee, J., Meyer, K.A., Prozesky, V.M. (2001), *Nucl. Instrum. Methods* **B181**, 122.

Pascual-Izarra, C., Reis, M. A., Barradas, N. P. (2006a), *Nucl. Instrum. Methods* **B249**, 780.

Pascual-Izarra, C., Barradas N. P., Reis, M.A. (2006b), *Nucl. Instrum. Methods* **B249**, 820.

Paul, H.and Schinner, A. (2001), *Nucl. Instrum. Methods* **B179**, 299.

Paul, H.and Schinner, A. (2002), *Nucl. Instrum. Methods* **B195**, 166

Pezzi, R.P., Wallace, R.M., Copel, M., Baumvol, I.J.R. (2005), *AIP CP* **788**, 571.

Pezzi, R.P., Grande, P.L., Copel, M., Schiwietz, G., Krug, C., Baumvol, I.J.R. (2007), *Surface Science* **601**, 5559.

Rauhala, E. (1984), *J. Appl. Phys.* **56**, 3324.

Rauhala, E. (1987), *J. Appl. Phys.* **62**, 2140.

Rauhala, E., Barradas, N. P., Fazinic, S., Mayer, M., Szilágyi, E., Thompson, M. (2006), *Nucl. Instrum. Methods* **B244**, 436.

Reis, M.A., and Alves, L.C. (1992), *Nucl. Instrum. Methods* **B68**, 300.

Ryan, C.G., Cousens, D.R., Sie, S.H., Griffin, W.L., and Suter, G.G. (1990), *Nucl. Instr. Meth.* **B47**, 271.

Ryan, C.G. (2000), *Int. J. Imaging Systems Technol.* **11**, 219.

SaariLahti J., Rauhala E., (1992), *Nucl. Instr. and Meth.* **B64**, 734.

Sajavaara, T., Jokinen, J., Arstila, K., Keinonen, J. (1998), *Nucl. Instr. and Meth.* **B139**, 225.

Smulders P.J.M., Boerma D.O. (1987), *Nucl. Instrum. Methods* **B29**, 471.

Spaeth, C. , Richter, F., Grigull, S. and Kreissig, U. (1998) , *Nucl. Instrum. Methods* **B140**, 243.

Szilágyi, E., Pászti, F., Amsel, G. (1995), *Nucl. Instrum. Methods*. **B100**, 103.

Szilágyi, E. (2000), *Nucl. Instrum. Methods* **B161-163**, 37.

“Handbook of Modern Ion Beam Materials Analysis“, (1995), Tesmer, J.R., and Nastasi M., eds, Materials Research Society, Pittsburgh.

Tosaki, M., Ito, S., and Maeda, N. (2000), *Nucl. Instrum. Methods* **B168**, 543.

Tschalär, C. (1968a), *Nucl. Instr. and Meth.* **61**, 141.

Tschalär, C. (1968b), *Nucl. Instr. and Meth.* **64**, 237.

Tschalär, C., Maccabee, H.D. (1970), *Phys. Rev.* **B1**, 2863.

Vickridge, I., and Amsel, G. (1990), *Nucl. Instrum. Methods* **B45**, 6.

Wielopolski, L. and Gardner, R.P. (1976), *Nucl. Instrum. Methods* **133**, 303.

Wielopolski, L. and Gardner, R.P. (1977), *Nucl. Instrum. Methods* **140**, 297.

Yang, Q., O'Connor, D.J., Wang, Z. (1991), *Nucl. Instrum. Methods* **B61**, 149.

Ziegler, J.F., Lever, R.F., and Hirvonen, J.K. (1976), in “Ion Beam Surface Layer Analysis, Vol. 1” (Meyer, O., Linker, G. and Käppeler, F., eds) , p. 163. Plenum, New York.

Ziegler, J.F. (2004), *Nucl. Instrum. Methods* **B219-220**, 1027.

“SRIM - The Stopping and Range of Ions in matter”, (2008), Ziegler, J.F., Biersack, J.P., and Ziegler, M.D., SRIM Co., Maryland, ISBN 0-9654207-1-X